Closing and opening holes in the glycan shield of HIV-1 envelope glycoprotein SOSIP trimers can redirect the neutralizing antibody response to the newly unmasked epitopes

Rajesh P. Ringe[1], Pavel Pugach[1], Christopher A. Cottrell[2], Celia C. LaBranche[3], Gemma E. Seabright[4], Thomas J. Ketas[1], Gabriel Ozorowski[2], Sonu Kumar[2], Anna Schorcht[5], Marit J. van Gils[5], Max Crispin[4], David C. Montefiori[3], Ian A. Wilson[2,6], Andrew B. Ward[2], Rogier W. Sanders[1,5], P. J. Klasse[1,#], John P. Moore[1,#]

[1] Department of Microbiology and Immunology, Weill Cornell Medical College, New York, NY 10021, USA
[2] Department of Integrative Structural and Computational Biology, IAVI Neutralizing Antibody Center and Center for HIV/AIDS Vaccine Immunology and Immunogen Discovery, The Scripps Research Institute, La Jolla, CA 92037, USA
[3] Department of Surgery, Duke University Medical Center, Durham, NC 27710, USA
[4] Biological Sciences & The Institute for Life Sciences, University of Southampton, Southampton SO17 1BJ, United Kingdom
[5] Department of Medical Microbiology, Academic Medical Center, University of Amsterdam, 1105 AZ Amsterdam, The Netherlands
[6] The Skaggs Institute for Chemical Biology, The Scripps Research Institute, La Jolla, CA 92037, USA

Corresponding authors' mailing addresses:

John P. Moore, Department of Microbiology and Immunology, Weill Medical College of Cornell University, New York, NY 10065, USA: Email: jpm2003@med.cornell.edu
P.J. Klasse, Department of Microbiology and Immunology, Weill Medical College of Cornell University, New York, NY 10065, USA: Email: pek2003@med.cornell.edu

Short title: Immunogenic epitopes on native-like HIV-1 trimers

Keywords: HIV-1 vaccine; neutralizing antibodies; Env trimers; epitopes

Word count Abstract: 239

Word count Importance: 133

Word count Text: 7600

Abstract

In HIV-1 vaccine research, native-like, soluble envelope glycoprotein SOSIP trimers are widely used for immunizing animals. The epitopes of autologous neutralizing antibodies (NAbs) induced by the BG505 and B41 SOSIP trimers in rabbits and macaques have been mapped to a few holes in the glycan shields that cover most of the protein surfaces. For BG505 trimers, the dominant autologous NAb epitope in rabbits involves residues that line a cavity caused by the absence of a glycan at residue 241. Here, we blocked this epitope in BG505 SOSIPv4.1 trimer immunogens by knocking-in an N-linked glycan at residue 241. We then opened holes elsewhere on the trimer by knocking-out single N-linked glycans at residues 197, 234, 276, 332 or 355, and found that NAb responses induced by the 241-glycan-bearing BG505 trimers were frequently re-directed to the newly opened sites. The strongest evidence for redirection of the NAb response to neo-epitopes, through the opening and closing of glycan holes, was obtained from trimer immunogen groups with the highest occupancy of the N241 site. We also attempted to knock-in the N289-glycan to block the sole autologous NAb epitope on the B41 SOSIP.v4.1 trimer. Although a retrospective analysis showed that the new N289-glycan site was substantially under-occupied, we found some evidence for redirection of the NAb response to a neo-epitope when this site was knocked-in and the N356-glycan site knocked-out. In neither study, however, was redirection associated with increased neutralization of heterologous Tier-2 viruses.

Importance

Engineered SOSIP-trimers mimic envelope-glycoprotein spikes, which stud the surface of HIV-1 particles and mediate viral entry into cells. When used for immunizing test animals they elicit antibodies that neutralize resistant sequence-matched HIV-1 isolates. These neutralizing antibodies recognize epitopes in holes in the glycan shield that covers the trimer. Here, we added glycans to block the most immunogenic neutralization epitopes on BG505 and B41 SOSIP trimers. In addition, we removed selected other glycans to open new holes that might expose new immunogenic epitopes. We immunized rabbits with the various glycan-modified trimers and then dissected the specificities of the antibody responses. Thus, in principle, the antibody response might be diverted from one site to a more cross-reactive one, which would help in the induction of broadly neutralizing antibodies by HIV-1 vaccines based on envelope glycoproteins.

Introduction

The development of soluble envelope glycoprotein (Env) trimers as vaccine candidates against human immunodeficiency virus type 1 (HIV-1) is predicated upon the induction of sustained protective neutralizing antibody (NAb) responses (reviewed in (1-8)). The BG505 SOSIP.664 construct is the prototype native-like recombinant Env trimer and has been widely used in recent years; SOSIP trimers based on BG505 and other HIV-1 *env* genes mimic the native structure of the Env spikes that mediate HIV-1-virion attachment to and entry into target cells (2, 9-18). These functionally critical processes are impeded by the binding of NAbs to the trimers (8, 15, 19-26). Knowledge of the immunogenicity of native-like trimers in general, in particular of the NAb responses they elicit, will help to refine vaccine development aimed at eventually inducing NAbs with broad activity against diverse HIV-1 strains (bNAbs) (1-3). The BG505 SOSIP.664 and other native-like trimers present multiple bNAb epitopes, but induce only a narrow NAb response in rabbits and macaques (14, 27-30). It is widely appreciated that antigenicity, i.e., recognition of an epitope by an immune response, is not the same as immunogenicity, i.e., the capacity to induce an immune response to an epitope. In addition, factors other than accessibility influence the bNAb response to an epitope (2, 3, 7, 22, 31, 32).

Previous studies have shown that BG505 SOSIP.664 trimers induce autologous NAbs against the Tier-2 BG505.T332N virus that target specific holes in the glycan shield, which covers most of the trimer surface (29, 33-42). The immunogenicity of such glycan-deficient patches was first shown with virus-like particles expressing trimers based on the JR-FL strain (40). Such epitopes also dominate the response to soluble SOSIP trimers of both the BG505 and B41 genotypes (29). Specifically, autologous NAbs induced by the BG505 SOSIP.664 trimer in rabbits most frequently recognize a hole in the glycan shield caused by the absence in that strain of a glycan at residue 241. Thus, the addition of a glycan at this position, or at the structurally nearby residues 289 or 230, renders the autologous BG505.T332N virus resistant to NAbs from most trimer-immunized rabbits (38). A second autologous NAb epitope, the C3/465 site, is seen less frequently by the rabbit but more often by the macaque immune system, and involves residues in the gp120 C3 and V5 regions. This epitope is blocked by the addition of glycans at residues 356 or 465. A third, rarely immunogenic, epitope is located in V1 near residues 133 and 136 (38). The B41 SOSIP.664 trimer also induces autologous NAbs in rabbits, which, in this case, are directed to a single epitope cluster that can be blocked by knocking-in a glycan at

residue 289 (29). Both of these trimers also elicit antibodies to the V3 and other regions, which neutralize only sensitive Tier-1 viruses (14, 29, 38). In addition, immunogenic neo-epitopes are created at the base of all soluble trimers, inducing non-neutralizing antibodies (non-NAbs) (43-45).

As noted above, the bNAb epitopes on SOSIP trimers have been immuno-silent in animal studies with intact trimers to date. Strategies to overcome this problem include trimers that are sequence-modified to target the germline-precursors of human bNAbs (6, 46-48). A related topic is whether immuno-dominant NAb or non-NAb epitopes distract the antibody response from the less immunogenic bNAb sites on the same trimer. Accordingly, multiple attempts have been made to reduce the immunogenicity of the V3 region of SOSIP trimers and, more recently, the neo-epitopes at the trimer base (9, 27, 30, 44, 49-51). Whereas suppression of the less desired responses against these epitopes can certainly be achieved, it has not been accompanied by meaningful improvements in autologous NAb titers or the emergence of more broadly active antibodies (45); whether eliminating the immunogenicity of non-NAb epitopes at the base of the soluble trimer is beneficial remains to be definitively determined. Another approach to neutralization breadth involved efforts to increase the immunogenicity of bNAb epitopes near the CD4 binding-site (CD4bs) by deleting one or more nearby epitope-shielding glycans from SOSIP trimers of BG505 and other genotypes (39). This outcome can be achieved with only a minimal impact on the processing state of nearby glycans (52). In immunogenicity studies, NAbs were indeed elicited that targeted epitopes in the newly opened holes in the glycan shields of the corresponding (sequence-matched) mutant viruses, but without the generation of CD4bs-related cross-neutralizing antibodies (39).

Here, we have explored a different but related strategy: blocking the known immunodominant autologous NAb epitopes on the BG505 and B41 SOSIP trimers, while opening up alternative holes in the glycan shield, to see whether new NAb epitopes are created. Accordingly, we produced variant BG505 trimers based on the SOSIP.v4.1 design (27). A blocking glycan was first added at residue 241 to reduce the immunogenicity of the 241/289-glycan hole epitope. This N241-knock-in (N241-KI) variant trimer was then used as the template for deleting glycans from residues 197, 234, 276, 332 or 355 to make glycan knock-out (KO) mutants. Using this panel of trimer variants as immunogens in rabbits, we found that it is indeed possible to reduce the immunogenicity of the immunodominant 241/289-glycan hole epitope

and, in some cases, to divert the NAb response to neo-epitopes in the newly opened holes. But we did not observe any increase in the breadth of neutralization against heterologous Tier-2 viruses. On the B41 SOSIP.v4.1 trimer, we knocked-in a glycan at residue 289 in an attempt to block the only known autologous NAb epitope, and then opened new glycan holes at residues 332 and 356. Unexpectedly, a retrospective analysis of glycan occupancy found that the residue 289 was variably but poorly occupied on the 289-KI mutant trimers. Hence, NAbs against this epitope were still induced in immunized rabbits. We did, however, find some evidence that an immunogenic neo-epitope was be created by knocking-out the N356-glycan, but not by knocking-out the N332-glycan. We note that a recent report shows that the development of neutralization breadth in HIV-1 infected people is correlated with the lack of glycan holes on the Env proteins of the initially infecting virus (53). In this context, the new information we describe here could be helpful for designing new immunogens with closed glycan holes as components of stratgeies to induce bNAbs.

Results

Design, production and use of glycan-modified SOSIP trimer immunogens

We based the design of the BG505 SOSIP.v4.1 trimer variants on our identification of the 241/289-glycan hole as the predominant autologous NAb epitope in rabbits (29). Accordingly, we knocked-in a glycan at residue 241 in an attempt to block access to this epitope. At the time this study was initiated, we had not identified the C3/465 epitope as the next-most immunogenic autologous NAb epitope (38). Hence, we did not change this site on the mutant trimers used in this study (although see the description of Group-8, below). For B41, we knocked-in a glycan at residue 289 in an attempt to close the only known epitope for autologous NAbs on this genotype of SOSIP trimer (13, 29). The amino-acid sequence changes and designations of the various trimers used in this study are described in A Tables 1 and 2. Data on the occupancy of the various knocked-in glycans are described below and were obtained by a proteomics-based method (37) only after the immunization experiments had been completed.

In our previous rabbit immunization studies, we used Iscomatrix adjuvant (14, 27, 29, 50, 54). However, as this reagent was no longer available, we obtained GLA-LSQ from the Infectious Disease Research Institute (IDRI), Seattle, WA via the Bill and Melinda Gates Foundation's (BMGF) collaborative network and used it for the first 4 immunizations. While this adjuvant did support the immunogenicity of the various BG505 and B41 SOSIP.v4.1 trimers, we were concerned that, in this and other contemporaneous experiments not reported here, the incidence of non- or poorly-responding rabbits was higher than we expected. For example, of the 5 rabbits immunized four times with the parental BG505 SOSIP.v4.1 trimers in GLA-LSQ, only 2 had autologous NAb titers >20 (specifically, 150 and 700), which corresponds to fewer responses and lower titers than we typically see after 3 immunizations with Iscomatrix (14, 27, 29, 50, 54) (see also the summary of Group-1 below). For the parental B41 SOSIP.v4.1 trimers, the autologous NAb titers after three or four immunizations with GLA-LSQ also tended to be lower than those previously obtained with Iscomatrix (14, 29, 54). In an attempt to increase the NAb responses, we re-boosted all the rabbits in every BG505 and B41 immunogen group twice with the same trimers and a different adjuvant, an Adjuplex-based formulation (see Methods). The response rate in the parental trimer and other groups then increased. Accordingly, the data presented below were all obtained 2 weeks after the sixth immunization (4 with GLA-LSQ and then 2 with the Adjuplex-based formulation).

The neutralization responses, including mapping data, are summarized below on a group-by-group basis for the BG505 trimers, and then for B41. For BG505, the data were derived with the parental BG505.T332N pseudovirus, mutants corresponding to the immunogen trimers and other mutants with substitutions at the 241/289 and C3/465 sites that are targeted by NAbs from most rabbits immunized with BG505 SOSIP trimers (29, 38). For B41, the data were obtained with the parental B41.R315Q and glycan site mutant pseudoviruses. In both cases, assessments of titer changes could only be made reliably when the ID_{50} values against the parental pseudovirus or the autologous, i.e., immunogen-matching, virus were >100.

Group-1: The parental BG505 SOSIP.v4.1 trimer

The neutralization data for all 8 of the BG505 trimer immunogen groups are summarized in Fig.1. The abilities of the sera to neutralize the autologous (trimer immunogen-matched) pseudovirus and the parental (BG505.T332N) pseudovirus are shown in Fig.1A and Fig.1B, respectively. For Group-1, the data are the same in both plots as the autologous virus is the parental.

After their sixth immunization, all the Group-1 rabbits developed detectable, albeit wide-ranging, autologous NAb titers, which was also the case for most of the other groups (Fig. 1A). For Group-1, sera from the 5 rabbits generated ID_{50} values in the range 51-5800 (median 140) against the autologous, parental pseudovirus (Fig.1A, B). Two sera, r2213-1 and r2214-1, neutralized this virus with high ID_{50} values of 640 and 5800, the other three with low ID_{50} values (Fig. 1). For both of the strongly neutralizing sera, the NAb titers were markedly reduced (relative ID_{50}, RID_{50}, values: 5-32%) by the N241-KI and N241-KI/N289-KI mutations, while the C3/465 epitope was not targeted (Fig.2A, B).

Group-2: The BG505 SOSIP.v4.1+ N241-KI trimer

The N241-KI trimer has a glycan inserted at residue 241 to block the dominant 241/289-glycan hole site (Fig.3A). Three out of 5 rabbits developed detectable but low NAb responses against the autologous N241-KI mutant pseudovirus (Fig.1A). The NAb titers against the parental BG505.T332N pseudovirus and the autologous responses against the N241-KI mutant pseudovirus in the Group-2 rabbits were indistinguishable and in the range 20-260; hence these weak responses tolerated the N241-KI mutation (Fig.1A and B; A Fig.1). These titers, both autologous and against the parental virus, were lower than the autologous responses in Group-1

(titers of 51-5800). It is, therefore, possible that the added N241-glycan had suppressed the immunogenicity of the trimer, although the statistical trend was not significant ($p = 0.14$ in both cases). Only one rabbit (r2220-2) developed NAbs that neutralized the parental pseudovirus at a titer (ID_{50} = 250) high enough for the cross-reactive epitope to be mapped. The reduced RID_{50} value of this serum for the N365-KI/R360I double mutant implicated the C3/465 site as the NAb target (Fig.3B).

Group-3: The BG505 SOSIP.v4.1 + N241-KI + N130-KI trimer

This mutated trimer contained knocked-in glycans at both residues 241 and 130, the latter to block a putative glycan hole in V1 (Fig.4A). The design of this immunogen was suggested by comparative sequence analysis and structural modeling; in the Los Alamos database, 62% of the isolates have a glycan at residue 130 (https://www.hiv.lanl.gov). The design of this trimer predated our use of BG505.T332N virus mutants to map NAb responses, which showed that the N130-KI mutation did not reduce ID_{50} values for sera from BG505 SOSIP.664 trimer-immunized rabbits (38). Four of the 5 rabbits developed detectable autologous NAb responses (20-1900; median = 82) (Fig.1A). In 2 of the animals, the responses against the parental virus were strong enough for the shared epitope to be analyzed (Fig.1B). For r2225-3, the NAb response in was clearly directed against the C3/465 site, but the evidence was less definitive for r2224-3 (Fig.4B). Here, however, we noted that the NAb titer against the autologous N130-KI/N241-KI mutant pseudovirus was increased by 72% compared with the parental (i.e., an RID_{50} of 172%) (Fig.4B). Hence, a partial redirection of the neutralization response to an immunogen-specific, glycan-dependent neo-epitope(s) may have occurred in this rabbit.

Group-4: The BG505 SOSIP.v4.1+ N241-KI + N197-KO trimer

In this group, the immunogen was a trimer with the N241-glycan knocked-in and the glycan at C2 residue 197 knocked-out (Fig.5A). This design was intended to answer whether the NAb response could be diverted from the 241/289-glycan hole epitope towards the lining of the hole that was created within C2 in proximity to the CD4bs. However, as the N241-KI + N197-KO double mutant virus was non-infectious, the analysis was restricted to the N197-KO mutant pseudovirus. The ID_{50} values against this mutant pseudovirus ranged from 39 to 15000 (median = 470) (Fig.1A). Three rabbits raised NAb responses that strongly cross-neutralized the parental BG505.T332N pseudovirus (Fig.1B). In sera r2228-4 and r2231-4, these NAbs were directed

against the C3/465 site (Fig.5B). However, the NAbs in r2229-4 were partly re-directed to a neo-epitope dependent on the N197-KO mutation (Fig.5B). The effect on NAb recognition of this change when combined with the N241-KI mutation could not be tested since that double mutant pseudovirus was not infectious.

One rabbit in Group-4 (r2228-4) produced a particularly strong pan-neutralizing response across all of the BG505-based pseudoviruses that it was tested against (Fig.5B). Against other mutants not included in Fig.5B, the ID_{50} values for this serum were in the range 4800-29000. The lower values occurred with viruses that included mutations in the C3/465 site, such as the N356-KI and N465-KI changes (Fig.5B). RID_{50} values against the N355-KO and N241-KI + N355-KO mutants were ~30%. We conclude that the N197-KO mutation had not created an immunogenic epitope in this rabbit and that the NAb response was directed to the C3/465 site, including the N355-glycan. It may or may not have been diverted there by the N241-KI mutation as this site is immunogenic in a subset of rabbits given the parental trimer (38).

Group-5: The BG505 SOSIP.v4.1+ N241-KI + N234-KO trimer

The immunogen had the N241-KI mutation and a new hole in the glycan shield at residue 234 that is close to the CD4bs (Fig.6A). The parental NAb titers in Group-5 were significantly lower than the autologous titers, suggesting that the responses in that group had been redirected ($p = 0.0079$, Fig.1A and B, A Fig.1). Thus, all 5 rabbits responded with substantial NAb titers (ID_{50} 1700, median = 800) against the autologous N241-KI + N234-KO mutant pseudovirus (Fig.1A), but none of the sera cross-neutralized the parental pseudovirus (Fig.1B). The consistently and markedly enhanced neutralization (RID_{50} 700-4100%) of the N234-KO and N241-KI + N234-KO mutant pseudoviruses by all 5 sera implies that a consistently immunogenic neo-epitope has been created by eliminating the N234-glycan from the trimer (Fig.6B).

Group-6: The BG505 SOSIP.v4.1 + N241-KI + N276-KO trimer

Here, the N241-KI mutation was accompanied by a newly opened hole at residue 276, where this CD4bs-flanking glycan was deleted (Fig.7A). Sera from 4 rabbits immunized with this trimer variant neutralized the autologous N241-KI + N276-KO mutant pseudovirus detectably (ID_{50} 20-1800, median 570) (Fig.1A), while 3 sera (r2237-6, r2241-6 and r2240-6)

strongly cross-neutralized the parental virus (Fig.1B). In rabbits r2237-6 and r2241-6, the NAbs were directed against the C3/465 site, but we were unable to identify the epitope on the parental pseudovirus that was targeted by NAbs in the r2240-6 serum (Fig.7B). For rabbits r2238-6 and r2240-6, the strongly enhanced neutralization (RID_{50} 950-6444%) of the N276-KO and N241-KI + N276-KO mutants clearly showed that NAbs were generated against the newly created N276-glycan hole (Fig.7B). It is possible that N276-KO mutation specifically facilitates the binding of antibodies with an approach angle similar to that of some CD4bs-targeting bNAbs, such as VRC01 and N6 (55, 56). Indeed, VRC01 was 14-fold and N6 was 10-fold more potent against the N276-KO mutant than the parental pseudovirus (the respective IC_{50} values were: VRC01, 0.014 ± 0.0011 *vs*. 0.19 ± 0.025 μg/ml; N6, 0.012 ± 0.0010 *vs*. 0.13 ± 0.0088 μg/ml).

Group-7: The BG505 SOSIP.v4.1+ N241+ KI + N332-KO trimer

Here, we tested the effect of knocking out the N332-glycan from the N241-KI mutant trimer (Fig.8A). All 5 of the resulting Group-7 sera neutralized the autologous N241-KI/N332-KO virus (ID_{50} 120-650, median 330) (Fig.1A) and 4 of them cross-neutralized the parental virus (Fig.1B). The responses in the 4 cross-reactive sera were directed against the C3/465 site, although the N289-KI mutation also had a modest additional effect (Fig.8B). Two of the rabbits (r2243-7 and r2246-7), however, also generated NAbs against the neo-epitope created by the N332-glycan deletion, as shown by the increased neutralization (RID_{50} 200-1500%) of the N332-KO and N241-KI + N332-KO viruses (Fig.8B).

*Group-8: The BG505 SOSIP.v4.1 + N241-KI + N355-KO trime*r

The final group received the N241-KI mutant trimer from which the N355-glycan was deleted (Fig.9A). The NAb titers against the autologous virus varied widely, but two rabbits responded strongly (Fig.1A). Four of the sera weakly neutralized the parental virus; the fifth was negative (Fig.1B). There was a non-significant trend for the titers against the autologous N241-KI + N355-KO virus to be higher than against the parental BG505.T332N virus ($p = 0.15$). The likely explanation for the low ID_{50} values is that the N355-KO mutation also changed the immune response to the C3/465 site, as residue 355 is located within a stretch of C3 residues that is integral to that epitope (38). (N.B., as stated above, we were unaware of the existence of this NAb epitope at the time the mutant trimer was designed, so this outcome was fortuitous). Hence,

on the SOSIP.v4.1 + N241-KI + N355-KO trimer immunogen, the principal immunogenic NAb epitopes are either blocked when the N241 glycan is knocked-in or affected when the N355 glycan is knocked-out. It was notable, however, that sera from 3 of the immunized rabbits (r2248-8, r2250-8 and r2249-8) had enhanced neutralization activity (RID_{50} 455-25000%) against the N355-KO and N241-KO + N355-KO viruses (Fig.9B). Thus, although the N355-KO mutation eliminated the cross-reactivity with the parental C3/465 epitope, it apparently also created an immunogenic neo-epitope. It seems, however, that the antibodies raised against this neo-epitope can only neutralize mutant viruses that also lack the N355-glycan. Four different N355-KO mutant pseudoviruses are resistant to neutralization by some sera from BG505 SOSIP.664 trimer-immunized rabbits that contain NAbs directed against the C3/465 epitope cluster (38). It is possible that the N355-glycan contributes to a subset of C3/465 region epitopes while a glycan resulting from the N356-KI mutation blocks access to all such epitopes (38). In contrast, neutralization by rabbit sera specific for the 241/289-glycan hole is frequently enhanced by the N355-KO mutations (38). An explanation may be the existence of an immunogenic trimer sub-population on which N355 glycan site is not occupied, and that induces antibodies that can only neutralize viruses lacking that glycan (38).

Overall neutralization sensitivity of glycan-KO and non-glycan KO mutants, Tier-1A NAb responses and evidence for redirection

The ID_{50} values for neutralization of glycan-KO mutant viruses by the non-autologous (i.e., group- and virus-mismatched) sera (n = 315) did not differ from those for neutralization of non-glycan-KO viruses by non-autologous sera (n = 140, p = 0.73). This analysis shows that the glycan-KO mutants had not become globally neutralization-sensitive. We then checked whether the glycan-KO mutant trimers (Groups 4-8) had induced stronger neutralization titers against Tier-1A viruses, MN.3 and MW965.26, than did the non-glycan-KO mutant trimers (Groups 1-3, A Fig.2). There was again no difference (p = 0.98 and p = 0.63 against MN.3 and MW965.26, respectively). We also found general evidence that NAb responses were redirected to epitopes in the newly opened glycan holes. Thus, serum ID_{50} values against the immunogen-matched glycan-KO mutant pseudoviruses (n = 45, median = 410) were significantly higher than against non-immunogen-matched glycan-KO mutants (n = 315, median = 66; p < 0.0001; A Fig.3).

Glycan occupancy on BG505 SOSIP.v4.1 trimers

An assumption underlying this experiment was that glycans would be added efficiently at each knocked-in potential N-linked glycosylation site (PNGS) on the SOSIP trimer immunogens and the corresponding mutant pseudoviruses. Recent efforts to measure glycan occupancy at specific sites on trimers and viruses have shown that the above assumption is not always valid; thus, a small subset of PNGS on SOSIP trimers of three different genotypes are significantly under-occupied (<90%), whereas occupancy approaches 100% across the glycan sites on virion-derived Env (37, 57, 58). We applied the latest methodology to retrospectively quantify glycan-site occupancy at the knocked-in sites on the BG505 SOSIP.v4.1 trimer immunogens. The N241 site was occupied to extents that varied from 81% (Group-4) to 100% (Group-5) on the various trimers for Groups 2-8, almost exclusively by oligomannose glycans (Fig.10A). For comparison, the N332 site was almost completely occupied (~100%) on the trimers used to immunize Groups 1-6 and 8, although the proportion of complex glycans varied from 2.2-14% (Fig.10A).

Every glycan site on a lymphoid cell line-derived stock of fully infectious BG505.T332N virus has been found to be almost fully occupied (58). We were not able to produce enough pseudovirus for occupancy analyses, but we analyzed the available neutralization assay data in two ways relevant to N241-glycan occupancy. First, we identified sera from 13 rabbits in Groups 2-8 for which the ID_{50} values against the parental BG505.T332N pseudovirus were >100; the RID_{50} values for those sera against the N241-KI mutant are listed in Figs.3-9. The ID_{50} values for these 13 sera against the N241-KI mutant and parental viruses were indistinguishable ($p = 0.67$, Wilcoxon's signed ranked test against the 100% RID_{50} value for the parental). Thus, the N241-KI mutation in the pseudovirus did not consistently reduce the titers, and for one Group-4 serum, r2241-4, the RID_{50} value for the mutant virus was even increased to 210%. These observations suggest that the dominant NAbs can bind at least as well in the presence of the N241-glycan as in its absence. Second, sera from all 17 rabbits in Groups 5-8 included in Figures 6-9, which received different N241-KI + glycan-KO mutant immunogens, had ID_{50} values > 100 against the corresponding single glycan-KO mutant. Those NAb responses were high enough to allow quantification of potential titer-reducing effects of the N241-KI mutation. But the titers against the double N241-KI + glycan-KO mutants did not differ significantly from those against the single glycan-KO mutants ($p = 0.24$, Wilcoxon's matched-pairs test).

Taken together, the above findings suggest that the N241 site was highly occupied on the various BG505 SOSIP.v4.1 trimer immunogens that include the N241-KI mutation and also on the corresponding N241-KI mutant pseudoviruses. The glycan-site occupancy data for the trimers are therefore consistent with the relatively strong neutralization, where measurable, of the N241-KI virus in Groups 2-8. However, the observed variation in occupancy of 81-100% among the immunogen groups could have consequences; a low level of non-occupancy might not confer neutralization sensitivity to a virus (59, 60), but the same degree of non-occupancy (e.g., 20% of the Env proteins) on an immunogen trimer might induce a dominant antibody response that neutralizes only viruses that lack the same glycan, either naturally or created by a KO-mutation. In this context, we note that the strongest evidence for redirection of the NAb response to neo-epitopes, through the opening and closing of glycan holes, was from the trimer immunogen groups with the highest occupancy of the N241 site (100% in Group-5 and 96% in Group-8; Figs. 6, 9 and 10A). Conversely, there were at most weak indications of a redirected NAb response in Group-4, where the N241 site occupancy, 81%, was the lowest measured among the trimer immunogens. We also observed that the N130 site was poorly occupied, 41%, on the BG505 SOSIP.v4.1-N241 + KI + N130-KI trimer used to immunize Group-3 rabbits, which would increase the difficulty of inducing N130 glycan-dependent NAbs (Figs.4 and 10A).

Immunogenicity of the B41 SOSIP.v4.1 trimers

All of the B41 trimer immunogens incorporated the R315Q change to eliminate proteolytic clipping within V3 but, for simplicity, we omit its mention in the descriptions below. The rabbit experiment was based on 4 groups of 5 animals: Group-9, B41 SOSIP.v4.1; Group-10, B41 SOSIP.v4.1 + N289-KI; Group-11, B41 SOSIP.v4.1 + N289-KI + N332-KO; Group-12, B41 SOSIP.v4.1 + N289-KI + N356-KO (A Table 2). All animals responded with detectable autologous neutralization except two in Group-12 (Fig.11A). Of note is that, for Group-10, the autologous NAb response (i.e., to the B41 N289-KI virus) was markedly lower than the cross-neutralization of the parental B41 virus (Fig.11A, B; ID_{50} values of 44-670, median 90, *vs*. 820-30000, median 4300, p = 0.0079). One explanation could be that the glycan site was poorly occupied on the immunogen trimer.

The occupancy of the knocked-in N289 site on B41 trimer immunogens is discussed below. The autologous NAb responses in Group-9 were, as expected, directed to the N289-glycan hole, as judged by the resistance of the B41 N289-KI virus to the sera (Fig.12). However,

unexpectedly, such resistance occurred also in the Group-10 and Group-11 rabbits, which all received trimer variants on which the N289-glycan was knocked-in to fill that hole (Figs.13 and 14). We also found that the B41 N230-KI mutant virus consistently tracked the resistance of the N289-KI mutant. These two glycan sites are highly proximate, such that a knocked-in glycan at either site can block the same hole in the glycan shield (38). In Group-12, there were some similarities with but also differences from the other three groups (Fig.15). Of the three responding rabbits, r2271-12 and r2275-12 developed NAbs to the 289-glycan hole and the response in r2273-12 was partially sensitive to the nearby N230-KI substitution. However, r2272-12 developed NAbs only against a neo-epitope created by the N356-KO change, while r2271-12 and r2273-12 also raised NAbs against that site as well as against the N289/N230-glycan hole epitope (Fig.15). These findings contrast with the lack of evidence from Group-11 that the N332-KO mutation at the base of V3 produced an immunogenic neo-epitope.

Glycan occupancy on the B41 SOSIP.v4.1 trimers

A retrospective glycan site occupancy analysis of the immunogens provided an explanation for the immunogenicity of the 289-glycan hole on trimers that contained the N289-KI mutation, i.e. Groups 10-12. Thus, the N289 site was occupied on only 64% of the Group-10 trimers, and it was even less occupied, at 18%, on the Group-11 immunogens. Only for Group-12 was occupancy of the N289 site high, at 82% (Fig.10B). Substantial sub-populations of trimers with the immunogenic N289-glycan hole present accounts for the NAb responses in these groups, particularly Groups-10 and -11. The differences between the Group-11 (no NAbs to the N332-KO neo-epitope) and Group-12 trimers (NAbs elicited against the N356-KO neo-epitope) might reflect either inherent differences in the immunogenicity of the two newly created glycan-hole epitopes, or the greater occupancy of the N289 site for Group-12 (82% *vs*. 18%). If the latter explanation is correct, it would argue for the necessity to substantially block the immunodominant N289-site when diverting the NAb response elsewhere.

Analyses of the neutralization data are consistent with the observations that the N289 site was poorly occupied on the B41 SOSIP.v4.1-N289-KI trimers. Thus, sera from the 12 rabbits with high enough titers against the B41 parental virus to detect a reduction (ID_{50} > 100 in parental column: all sera except r2272-12 in Figs.12-15) had significantly lower RID_{50} values against the B41 N289-KI pseudovirus than against the parental ($p = 0.0005$, Wilcoxon's signed-

412 ranked test against the 100% RID_{50} of the parental). Furthermore, for sera with ID_{50} values >100
413 against the single glycan-KO mutants (all 8 sera included in Figs.14-15), the corresponding
414 values against the double N289-KI + glycan-KO mutants were significantly lower ($p = 0.0078$,
415 Wilcoxon's matched-pairs test).

416 *Neutralization assays with heterologous Tier-2 viruses*

417 All 40 of the BG505 trimer immunogen sera were tested against a global panel of 9 Tier-
418 2 pseudoviruses (61). Of the 360 combinations of rabbit sera and pseudoviruses, 60 yielded
419 background-corrected ID_{50} values >40, but only two of them exceeded 100 (A Fig.4A). The
420 frequency of ID_{50} values >40 differed among immunization groups and viruses, but there was no
421 identifiable concurrence between the absence or presence of a glycan on the trimer immunogens
422 and the pseudoviruses (A Fig.5).

423 The B41 trimer immunogen sera were tested against the same global panel of 9 Tier-2
424 pseudoviruses (61) (A Fig.4B). Somewhat higher titers were recorded than in the BG505
425 experiment ($p = 0.0002$, although the median ID_{50} values were <20 in both cases). Of the 180
426 serum-virus combinations, 19 gave ID_{50} values >40 (50-550). The strongest and most consistent
427 hits againt the Tier-2 viruses were recorded for rabbit r2257-9 from Group-9, which was
428 immunized with the parental B41 trimer. The virus most frequently neutralized was Ce1176 (7 of
429 20 sera with ID_{50} >40, range 50-550). Although viruses Ce1176 and X1632 both lack a glycan at
430 the exact N356 position (they have others nearby, A Fig.5), they were not detectably neutralized
431 by the Group-12 sera from rabbits immunized with the N356-KO trimer.

432 Thus, although there were indications that the B41 trimers may be somewhat superior to
433 their BG505 counterparts at inducing sporadic heterologous cross-neutralizing antibodies, the
434 glycan-KI and –KO mutations did not enhance neutralization breadth in either experiment.

435 **Discussion**

436 The autologous NAb responses elicited by BG505 SOSIP trimers in rabbits and rhesus
437 macaques are directed against epitopes in holes in the glycan shield, which normally hinders
438 elicitation of antibodies to much of the surface of the Env complex (29, 38). Epitopes located in
439 glycan holes are immunogenic also on the JR-FL, B41 and CZA97 trimers and may be generally
440 so (29, 40). The most immunogenic autologous NAb epitope clusters on the BG505 SOSIP
441 trimer and the corresponding virus have now been identified. The first is created by the absence

of glycans from residues 241 and 289 (the 241/289-glycan hole), and can be blocked by knocking-in a glycan at either position. The second, known as the C3/465 site, includes a stretch of residues in C3 and can be blocked by knocking-in a glycan at residue 356 or 465 (38). A third, less frequently recognized, epitope is located in the V1 region near residues 133 and 136 (38). In addition, several epitopes, principally involving the V3 region and the CD4- and co-receptor- binding site, are targeted by antibodies that neutralize only Tier-1 viruses, while neo-epitopes on the base of SOSIP trimers elicit non-NAbs (9, 27, 30, 43, 44, 49-51). The induction of Tier-1A NAbs, particularly to V3 epitopes, can be blocked to various extents by sequence changes in the SOSIP trimer, including those in the BG505 SOSIP.v4.1 variant on which the present study was based (9, 27, 49-51). However, reducing the immunogenicity of various "off-target" sites has not meaningfully increased the magnitude of the autologous NAb response or allowed more broadly reactive NAbs to be induced (45).

Here, we have explored a different but conceptually related theme involving glycan holes: does blocking an immunodominant glycan-hole autologous epitope divert the NAb response to new epitopes that are made accessible by deleting glycans elsewhere on the trimer immunogen? The relevance of this question is highlighted by a recent report that neutralization breadth is more likely to emerge when people are initially infected with HIV-1 strains that lack glycan-hole targets for an autologous NAb response (53). Accordingly, we produced a set of BG505 SOSIP.v4.1 trimers containing the N241-KI change to occlude the 241/289-glycan hole and with various other glycans knocked-out to create potential alternative targets. When these immunogens were designed, we were unaware of the immunogenicity of the C3/465 site, so we did not design sequence changes to block it. However, the N355-KO change in the Group-8 trimers is, fortuitously, located within that site.

Our study of these BG505 mutant trimers establishes that it is possible to reduce or even eliminate the immunogenicity of the 241/289-glycan-hole epitope. This conclusion is reached by two comparisons. First, introducing the N241-KI mutation in the BG505.T332N parental virus reduced the ID_{50} values >2-fold for Group-1 sera, but not for sera from Groups 2-8. Second, in Groups 5-8, the ID_{50} values for the single glycan-KO mutant viruses did not differ significantly from those for the double N241-KI + glycan-KO mutants, and in only 2 of the 17 cases were the ID_{50} values against the viruses containing the N241-KI mutation reduced >2-fold. We also found

that immunogenic neo-epitopes can be created by deleting glycans from selected positions and thereby opening up holes in the glycan shield. This was the apparent outcome for the glycans normally present at N197 (1 of 5 rabbits), N234 (5 of 5), N276 (2 of 5), N332 (2 of 5) and N355 (3 of 5). NAbs against the subdominant C3/465 epitope cluster were also induced in addition to, or instead of, the other redirected responses. These redirections may compete, and it may be desirable to suppress the immunogenicity of the C3/465 epitope cluster through targeted sequence changes to SOSIP trimer immunogens that, in addition, have the N241-KI mutation.

In the B41 study, we did not expect that the knocked-in N289-glycan site would be un-occupied on such a high, and also variable, proportion of the mutant B41 SOSIP trimers; this outcome was revealed by a retrospective analysis of the immunogens by a proteomics-based method (37). It is possible that the higher occupancy of the N241-KI site on the BG505 trimer than on the N289-KI site on its B41 counterpart might be explained by the higher number of N-linked glycan sites preceding the knocked-in site in the B41 than in the BG505 amino-acid sequence, i.e., 14 *vs*. 9. This higher density of glycans could limit substrate availability and thereby reduce the efficicacy of the glycosyltranserase. Whatever the explanation, NAbs to the N289-glycan hole were elicited in response to substantial sub-populations of B41 trimers on which this hole was not blocked. We did, however, see a NAb response to the neo-epitope created by the N356-KO mutation, whereas the N332-KO change had no such effect. The different outcomes of these two glycan-KO changes may reflect the different efficiencies with which the immunodominant N289-glycan hole was blocked on the two trimers, i.e., 82% for the N356-KO mutant but only 18% for its N332-KO counterpart. It is also possible that the two newly opened glycan holes have inherently different immunogenicities attributable to their linings and environments on the trimer.

In both the BG505 and the B41 studies, we found that re-directing NAb responses to neo-epitopes was favored by a relatively high occupancy of the knocked-in glycan site (N241-KI and N289-KI, respectively). Increasing the efficacy with which the immunodominant glycan hole is blocked may therefore be beneficial to this strategy. Sporadic neutralization of heterologous viruses was observed at low levels in both experiments, somewhat more so with the B41-trimer immunogens. The strongest and most consistent cross-neutralizing response was seen in a rabbit that received the parental B41 trimer, which we consider an anecdotal outcome. Thus, although the autologous NAb responses were diverted to neo-epitopes in some rabbits, in neither

503 experiment were such outcomes associated with the emergence of neutralization breadth. While
504 such an outcome would have been welcome, it was not expected. The goal of the experiment was
505 to garner knowledge on whether and how the NAb response to SOSIP trimers could be
506 manipulated and thereby inform future immunogen design. For example, if our germline-
507 targeting BG505 SOSIP.v4.1-GT1.1 trimer succeeds in triggering gl-bNAb lineages, we will
508 need to learn how to nurture such responses towards breadth by boosting with specifically
509 designed trimer variants (2, 6, 46-48). In this context, suppressing the immunogenicity of non-
510 NAb epitopes, the 241/289-glycan-hole epitope and, now its existence is known, the C3/465 site
511 may help to focus antibody responses on bNAb epitopes that involve small and relatively
512 conserved defects in the glycan shield.

513

Materials and Methods

Production and characterization of BG505 and B41 SOSIP.v4.1 trimer mutants

The BG505 mutants were all based on the SOSIP.v4.1 design that contains the E64K and A316W substitutions to the original SOSIP.664 sequence, to further stabilize the trimers and suppress the immunogenicity of non-NAb epitopes (14, 27). The B41 mutants were likewise based on the SOSIP.v4.1 design, but also contained an R315Q substitution in V3 to eliminate a low level of proteolytic clipping of this region that can occur with clade B trimers (13). For both genotypes, the trimers also contained a C-terminal D7324 epitope-tag. The substitutions used to knock-in and knock-out various glycan sites are listed in A Tables 1 and 2. Site-directed mutagenesis was performed by the QuikChange (Agilent Technologies) method, as described previously (51). For both genotypes, the trimers were expressed by transient transfection of 293F cells followed by PGT145 bNAb-affinity chromatography (13, 15). Each PGT145-purified variant trimer was verified to be >90% native-like when visualized by negative-stain electron microscopy, as described previously (15, 51, 62).

Immunization of rabbits

Female New Zealand White rabbits were immunized intramuscularly with 30 μg of the BG505 or B41 SOSIP.v4.1 trimer variants essentially as described previously but with the exceptions outlined below (14, 27, 29). Four immunizations were carried out at weeks 0, 4, 20 and 40 (for BG505), or 38 (for B41), each involving the GLA-LSQ adjuvant obtained from IDRI, Seattle, WA via the BMGF's collaborative network. The rabbits were then re-boosted at weeks 67 and 71 with the same trimers in an adjuvant formulation based on the Adjuplex product that was obtained as a gift from Dr. Cheng Cheng at the Vaccine Research Center of the National Institutes of Health, Bethesda, MA (63-65). Sera were obtained for analysis 2 weeks after each immunization. The data presented were derived from sera obtained at week 73, i.e., 2 weeks after the sixth immunization.

Ethics statement

The rabbit immunization study was approved and carried out in accordance with protocols provided to the Institutional Animal Care and Use Committee (IACUC) at Covance Research Products (CRP) Inc. (Denver, PA), study number C0026-17. The rabbits were housed, immunized and bled in compliance with the Animal Welfare Act and other federal statutes and

544 regulations relating to animals, and in adherence to the Guide for the Care and Use of Laboratory
545 Animals, National Research Council, 1996.

546 *Glycan site occupancy determinations*

547 A proteomics-based method was used to quantify the occupancy (and proportion of
548 oligomannose- and complex-type glycans) of N-linked glycans on the BG505 and B41
549 SOSIP.v4.1 trimer mutants (37). Briefly, glycopeptides were sequentially treated with Endo H
550 and PNGase F in the presence of ^{18}O-labelled water. The masses of the resulting peptides are
551 specific to each glycan type or reflect non-occupancy of the relevant site, thus allowing the
552 extent of occupancy to be quantified. These analyses were performed after completion of the
553 rabbit immunization experiments described above.

554 *Production and use of BG505.T332N and B41 Env-pseudotyped virus mutants*

555 Mutant BG505 *env* genes containing glycan site substitutions to match those in the
556 various SOSIP trimer immunogens were made as previously described (13-15) (A Table 3). The
557 BG505.T332N virus with a full-length cytoplasmic tail was used as the parental for mutant
558 design, as it contains a knocked-in N332 glycan to match its sequence with the corresponding
559 trimer immunogens (14, 15, 29). The B41 virus mutants are described in A Table 4. All these
560 viruses contain the R315Q substitution in V3; i.e. the B41.R315Q Env sequence was the parental
561 for the other mutant viruses. The infectivity of each Env-pseudovirus for Tzm-bl cells was
562 determined by titration. The dilution factors of the mutant pseudoviruses relative to that of the
563 parental yielding infectivity signals of ~ 10^5 cps are given in A Tables 3 and 4.

564 Neutralization of pseudoviruses was quantified in the TZM-bl cell assay, as described
565 previously (13-15); rabbit sera were analyzed at Duke University Medical Center (DUMC), a
566 subset of them also at the Academic Medical Center, Amsterdam (AMC), and monoclonal
567 antibodies (MAbs) at Weill Cornell Medical College (WCMC). The dilution factors reducing
568 infectivity by 50% (half-maximal inhibitory dilution factor, ID_{50}) for each pseudovirus and the
569 relative dilution factors (RID_{50}) for mutants compared with the parental BG505.T332N or
570 B41.R315Q pseudovirus, as reported in the Results section, were obtained as described
571 elsewhere (38). These values are based on two intra-assay replicates and the requisite repeats of
572 the assay to fulfill the following criteria: the average RLU (relative light unit) values of virus
573 control wells is >10 times the average RLU of cell control wells; the coefficient of variation (%)

574 between RLU in the virus control wells is ≤30%; the percent difference between duplicate wells
575 is ≤30% for sample dilutions that yield at least 40% neutralization; neutralization curves cross
576 the 50% neutralization value on the y axis 0 or 1 times; ID_{50} values based on sigmoid-curve fits
577 and linear interpolation between the two data points on either side of 50% are within 3-fold of
578 each other; and the value of the positive control (NAb) is within a 3-fold range of the established
579 mean. The rabbit sera were also tested against a panel of 9 Tier-2 pseudoviruses, as previously
580 described (61). The ID_{50} values against murine leukemia virus (MLV) were subtracted from
581 those for the test viruses to control for any cytoxicity.
582 *Structural modeling*
583 The three-dimensional model of the BG505 SOSIP.v4.1 trimer was based on the PDB-
584 5V8M crystal structure (66). The gp120 glycans were modeled as $Man_5GlcNAc_2$; gp41 glycans
585 were either derived from PDB-5FUU or modeled as Man_5 $GlcNAc_2$ (67). The three-dimensional
586 model of the B41 SOSIP.v4.1 trimer was based on an unpublished crystal structure of B41
587 SOSIP.664 at 3.5 Å (PDB-6MCO). BG505 models were visualized by UCSF Chimera (68), B41
588 models by Pymol (Schrödinger LLC, USA).
589 *Statistics*
590 Groups of rabbits were compared pairwise by the two-tailed Mann-Whitney U test. The
591 effects of mutations on neutralization by the respective sera were first compared by the Wilcoxon
592 matched-pairs test. If the pairing was not significant, as assessed by Spearman correlations, they
593 were then compared by Mann-Whitney U tests (used unless otherwise stated). The relative
594 neutralization of N241-KI mutants of BG505 and N289-KI mutants of B41 was compared with
595 the neutralization of parental virus, defined as 100%, by the Wilcoxon signed-rank test (all in
596 Prism, Graphpad).
597
598
599
600
601
602
603
604

Appendix

We compared neutralization of autologous and parental BG505.T332N pseudoviruses in Groups 2-8 (parental and autologous being the same in Group 1). In Groups 2 and 3, which received immunogens without glycan-KO mutations, the titers tended to be similar against autologous and parental viruses, demonstrating acceptance of the glycan-KI mutations by the Ab responses in those groups. The neutralizing titers tended to be higher against the autologous than the parental virus in the groups with glycan-KO mutation in the immunogen, i.e., Groups 4-8 (the virus in Group 4 being only near-autologous because the double mutant corresponding more closely to the immunogen was non-infectious, see main Figure 1). This difference was significant in Group 5 ($p = 0.0079$). Those findings suggest redirection of the responses to the epitopes unmasked by the glycan-KO mutations (A Fig.1).

Evidence for redirection of the responses was also obtained by another comparison. As shown in A Fig.3, the titers against pseduoviruses with glycan-KO mutations matching those in the immunogen were significantly higher than in the groups with non-matching glycan-KO mutations ($p = 0.0001$, A Fig.3).

As part of the characterization of the neutralizing responses in both the BG505 and B41 studies we determined the neutralization titers against two Tier-1A and nine Tier-2. The titers against the Tier-1A pseduoviruses MN.3 and MW965.26 were weak or moderate, as expected for immunogens with the stabilizing v4.1 mutations, which restrict the V3 immunogenicity that is largely responsible for the Tier-1 neutralization (A Fig.2, (27)).

Heterologous neutralization of Tier-2 viruses by the rabbit sera was sporadic and with a few exceptions in B41 groups weak. Notably, no relationship between the detectable neutralization of pseudoviruses in the Tier-2 panel or its strength, on the one hand, and glycan-defect similarities between immunogens and pseudoviruses, on the other, was discernable (A Fig.4). The alignments of the B41, BG505 and the Tier-2 panel Env sequences in the regions around mutated PNGS illustrate this lack of coincidence between positive neutralization and PNGS patterns in immunogen and pseudovirus (A Fig.5).

Acknowledgements

We are grateful to Erik Francomano, Gargi Debnath and Amanda Eaton for expert technical assistance. We thank Dr. Cheng Cheng of the NIAID Vaccine Research Center for the gift of an Adjuplex-based adjuvant. The non-animal research was supported by National Institutes of Health (NIH) grants P01 AI110657 (JPM, IAW, ABW, PJK, RWS) and R37 AI036082 (JPM and PJK), the NIH-NIAID NHP Humoral Immunology Laboratory Contract HHSN272201800004C (CCL and DCM) and Bill and Melinda Gates Foundation through the Collaboration for AIDS Discovery (OPP1115782 to M.C.). The animal studies were supported by the Bill and Melinda Gates Foundation grants OPP1132237 (JPM, RWS). CAC is supported by NIH F31 Ruth L. Kirschstein Predoctoral Award Al131873 and by the Achievement Rewards for College Scientists Foundation. The funders had no role in study design, data collection or interpretation, nor in the decision to submit the work for publication.

649 **Figure legends**
650
651 **Figure 1. Neutralization of the parental BG505.T332N and immunogen-autologous viruses**
652 In each panel, the ID_{50} values (y-axis) for sera from individual rabbits from the are arranged by
653 BG505 SOSIP.v.4.1 trimer immunogen group (see Results). The median value in each group is
654 indicated by the horizontal bar. Only sera with ID_{50} values >100 against the autologous or
655 parental virus could be mapped precisely against mutant pseudoviruses (see subsequent figures).
656 (**A**) Neutralization of the mutant pseudoviruses that are sequence-matched (autologous) to the
657 SOSIP trimer immunogens with respect to the glycan-KI and glycan–KO changes. The * for
658 Group-4 signifies that the N241-KI + N197-KO double mutant virus was non-infectious; the data
659 shown are for the N197-KO mutant. **(B)** Neutralization of the parental BG505.T332N
660 pseudovirus.
661
662 **Figure 2. Mutations affecting neutralization by Group-1 sera (parental BG505 SOSIP.v4.1**
663 **trimer immunogen)**
664 The layout of this figure applies to each of Figs. 2-9 and 12-15 with the exceptions noted in those
665 legends. (**A**) A surface-rendered model of the BG505 SOSIP.v4.1 trimer seen from the side, in
666 two different orientations, with the apex up (top images) or viewed from above (lower image). In
667 the subsequent figures, the orientation that most clearly displays the relevant glycan mutation is
668 used. The peptidic surface is colored light blue on one of the protomers and grey on the other
669 two (on some views not all three protomers are visible). The glycans are colored light green. The
670 model is based on PDB-5V8M. (**B**) The data shown are the ID_{50} values against the parental
671 BG505.T332N virus and the RID_{50} values (%) for neutralization of the indicated mutant
672 pseudoviruses by the rabbit sera listed on the left. The RID_{50} value = ((ID_{50} against mutant)/(ID_{50}
673 against parental) x 100%) and hence, by definition, is 100% for the parental pseudovirus. The
674 RID_{50} cells are color-coded as outlined in the key above the data panel. Intermediate and strong
675 neutralization resistance is shown in yellow or red, respectively, while increased neutralization
676 sensitivity is in blue. The Env mutations are indicated in the top row, and the complete sequence
677 changes in the mutants are listed in A Tables 1 and 2. RID_{50} values were only determined when
678 the ID_{50} values against the parental or autologous pseudovirus were >100. KI = glycan knock-in,

679 KO = glycan knock-out. ID_{50} and RID_{50} values >10 are rounded off to two significant digits and
680 those <10 to integers.
681
682 **Figure 3. Mutations affecting neutralization by Group-2 sera (BG505 SOSIP.v4.1 + N241-**
683 **KI trimer immunogen)**
684 The layout in panel **A** is analogous to that of Fig.2A, except that residue S241 (left) and the
685 glycan knocked-in at residue 241 (right) are both colored yellow on the light blue protomer. The
686 left image shows the hole that the new glycan blocks. The layout of panel **B** is analogous to that
687 of Fig.2B, where the color code is explained.
688
689 **Figure 4. Mutations affecting neutralization by Group-3 sera (BG505 SOSIP.v4.1 + N241-**
690 **KI + N130-KI trimer immunogen)**
691 The color coding of the protomers and glycans of the trimers, seen from above, in panel **A** is as
692 in Fig.2A, except that residue 130 (left) and the glycan knocked-in at residue 130 (right) are both
693 colored yellow. The left image shows the hole that the new glycan blocks. Note that the glycan
694 knocked-in at residue 241 is not visible since the trimer is viewed from above. The layout of
695 panel **B** is analogous to that of Fig.2B, where the color code is explained.
696
697 **Figure 5. Mutations affecting neutralization by Group-4 sera (BG505 SOSIP.v4.1 + N241-**
698 **KI + N197-KO trimer immunogen)**
699 The layout in panel **A** is analogous to that of Fig.2A, except that the glycan knocked-in at residue
700 241 is colored yellow on both images; the N241 glycan is partly covered by the N355 glycan in
701 light green. The glycan normally present at residue 197 (left image) and residue 197 itself (right
702 image) are both colored red to illustrate the hole created by the N197-KO mutation. The N355
703 glycan (light green) partly obscures the view of the N241 glycan, as in Fig.5-7 and 9. The layout
704 of panel **B** is analogous to that of Fig.2B, where the color code is explained. Note that the
705 immunogen-matched N241-KI + N197-KO double mutant virus was non-infectious.
706
707
708

Figure 6. Mutations affecting neutralization by Group-5 sera (BG505 SOSIP.v4.1 + N241-KI + N234-KO trimer immunogen)

The layout in panel **A** is analogous to that of Fig.5A. The glycan knocked-in at residue 241 is colored yellow on both images and the glycan knocked-out at residue 234 (left image) and residue 234 itself (right image) are both colored red, to illustrate the hole created by the N234-KO mutation. The layout of panel **B** is analogous to that of Fig.2B, where the color code is explained.

Figure 7. Mutations affecting neutralization by Group-6 sera (BG505 SOSIP.v4.1 + N241-KI + N276-KO trimer immunogen)

The layout in panel **A** is analogous to that of Fig.5A. The glycan knocked-in at residue 241 is colored yellow on both images and the glycan knocked-out at residue 276 (left image) and residue N276 (right image) are both colored red, to illustrate the hole created by the N276-KO mutation (i.e., by the T278A substitution). The layout of panel **B** is analogous to that of Fig.2B, where the color code is explained. The four cells to the right for r2238-6 are open because the ID_{50} value against the parental virus was < 100 and, hence, too low for precise mapping.

Figure 8. Mutations affecting neutralization by Group-7 sera (BG505 SOSIP.v4.1 + N241-KI + N332-KO trimer immunogen)

The layout in panel **A** is analogous to that of Fig.5A. The glycan knocked-in at residue 241 is colored yellow on both images and the glycan knocked-out at residue 332 (left image) and residue 332 itself (right image) are both colored red, to illustrate the hole created by the N332-KO mutation. The layout of panel **B** is comparable to that of Fig.2B, where the color code is explained. Four cells are open for r2243-7 because the ID_{50} value against the parental virus was < 100, and hence too low for precise mapping.

Figure 9. Mutations affecting neutralization by Group-8 sera (BG505 SOSIP.v4.1 + N241-KI + N355-KO trimer immunogen)

The layout in panel **A** is analogous to that of Fig.5A. The glycan knocked-in at residue 241 is colored yellow on both images and the glycan knocked-out at residue 355 (left image) and

739 residue 355 (right image) are both colored red, to illustrate the hole created by the N355-KO
740 mutation. The N355 glycan partly covers the N241 glycan in this view. The layout of panel **B** is
741 analogous to that of Fig.2B, where the color code is explained.
742
743 **Figure 10. Proteomics-based quantification of glycan occupancy at glycan-KI sites on**
744 **SOSIP trimers.** (**A**) The three diagrams show the proportions (y-axes) of the N130, N241 or
745 N332 sites occupied by oligomannose glycans (green) or complex-type glycans (pink) or not
746 occupied (grey) for the BG505 SOSIP.v4.1 trimer immunogens listed on the category axis. (**B**)
747 As for panel A, except the data are for the N289, N332 or N356 sites on the B41 SOSIP.v4.1
748 trimer immunogens. For both panels, the error bars represent s.e.m. for multiple peptides per site.
749 N/A = Not Applicable; i.e., the site was naturally absent or had been knocked-out.
750
751 **Figure 11. Neutralization of the parental B41.R315Q and immunogen-autologous viruses**
752 In each panel, the ID_{50} values (y-axis) for sera from individual rabbits are arranged by B41
753 SOSIP.v4.1 trimer immunogen group (see Results). The median value in each group is indicated
754 by the horizontal bar. Only sera with ID_{50} values >100 against the autologous or parental virus
755 could be mapped with any precision against mutant pseudoviruses (see subsequent figures). (**A**)
756 Neutralization of the mutant pseudoviruses that are sequence-matched (autologous) to the SOSIP
757 trimer immunogens in respect of the glycan-KI and glycan–KO changes. **(B)** Neutralization of
758 the parental B41.R315Q pseudovirus.
759
760 **Figure 12. Mutations affecting neutralization by Group-9 sera (parental B41 SOSIP.v4.1**
761 **trimer immunogen)**
762 (**A**) Surface-rendered model of the B41 SOSIP.v4.1 trimer seen from the side in two different
763 orientations, with the apex up (top images) or (lower image) viewed from above. The peptidic
764 surface is colored light blue on one of the protomers, grey on the other two (on some views not
765 all the protomers are visible). The glycans are colored light green on all three. The model is
766 based The three-dimensional model of the B41 SOSIP.v4.1 trimer was based on an unpublished
767 crystal structure of B41 SOSIP.664 at 3.5 Å (PDB-6MCO). The layout of panel **B** is analogous
768 to that of Fig.2B, where the color code is explained, except that the parental virus is B41.R315Q.
769

Figure 13. Mutations affecting neutralization by Group-10 sera (B41 SOSIP.v4.1 + N289-KI trimer immunogen)

The layout in panel **A** is analogous to that of Fig.2A, except that residue N289 (left) and the glycan knocked-in at residue 289 (right) are both colored yellow on the light blue protomer. The left image shows the hole that the new glycan blocks. The E290 and Q344 residues partly cover N289. The layout of panel **B** is analogous to that of Fig.2B, where the color code is explained.

Figure 14. Mutations affecting neutralization by Group-11 sera (B41 SOSIP.v4.1 + N289-KI + N332-KO trimer immunogen)

The layout in panel **A** is analogous to that of Fig.5A. The glycan knocked-in at residue 289 is colored yellow on both images and the glycan knocked-out at residue 332 (left image) and residue 332 (right image) are both colored red, to illustrate the hole created by the N332-KO mutation. The layout of panel **B** is analogous to that of Fig.2B, where the color code is explained.

Figure 15. Mutations affecting neutralization by Group-12 sera (B41 SOSIP.v4.1 + N289-KI + N356-KO trimer immunogen)

The layout in panel **A** is analogous to that of Fig.5A. The glycan knocked-in at residue 289 is colored yellow on both images and the glycan knocked-out at residue 356 (left image) and residue 356 (right image) are both colored red, to illustrate the hole created by the N356-KO mutation. The N356 glycan appears small because only its GlcNac component is shown. The layout of panel **B** is analogous to that of Fig.2B, where the color code is explained.

A Figure legends

A Figure 1. Comparison of neutralization of autologous and parental pseudoviruses. In each of the groups with non-parental BG505 SOSIP.v4.1 immunogens (Groups 2-8), the ID_{50} values for neutralization of autologous and parental pseudoviruses are compared. Above each group designation (group number and mutations in the immunogen) a short line represents individual rabbits and connect the ID_{50} value against the autologous (or near-autologous) virus at its left end with the corresponding value against the parental virus at its right end. In Group 2 the lines for two negative sera superimpose ($ID_{50} \leq 20$). Except in Group 2 and 3, i.e., those groups without glycan-KO mutations in the immunogen, many of the lines have downward slopes, indicating redirection to epitopes unmasked by the mutations. This tendency was significant in Group 5.

A Figure 2. Neutralization of Tier-1A viruses by rabbit sera. The ID_{50} values against the Tier-1A pseudoviruses MN.3 (left) and MW965.26 (right) are depicted above the respective group designations (group number and mutations in the immunogen) for the BG505 SOSIP.v4.1 immunization Groups 1-8 (**A**) and the B41 SOSIP.v4.1.R315Q immunization Groups 9-12 (**B**).

A Figure 3. General evidence for redirection to glycan-KO neo-epitopes. The ID_{50} values against the immunogen-matching glycan-KO mutant pseudoviruses (blue symbols, left column; n = 45) were compared with those against non-immunogen-matching glycan-KO mutants (red symbols, right column; n = 315). The matching serum-virus combinations had significantly higher ID_{50} values than the non-matching ones ($p < 0.0001$).

A Figure 4. Heterologous neutralization of Tier-2 viruses by rabbit sera. The sera from the BG505 Groups 1-8 (**A**) and the B41 Groups 9-12 (**B**) studies were tested against a standard global panel of 9 Tier-2 viruses (61). The titers (ID_{50} values) were determined in the Tzm-bl assay. All background-corrected ID_{50} values >40 (see Methods) are marked in blue and bold, values in the range 21-40 are in black, and values ≤20, regarded as negative, are represented by a hyphen-minus. The data for the BG505 study were determined at DUMC. For the B41 study, the sera were first tested at DUMC and then at the AMC. Sera from the three rabbits with the highest responses (2257-9, 2267-11 and 2268-11) were also re-tested at DUMC. The concordance

between the two centers in positive and negative results was >90%. The values in **B** are thus the means of 2-3 independent assays. (For intra-assay replicates and controls, see Methods). The absence (-) or presence (+) of glycan sites that correspond to some sites that are mutated in the BG505 and B41 SOSIP.v4.1 trimer immunogen groups is indicated under the virus designations. The BG505 SOSIP.v4.1 trimer immunogens for Groups 2-8 all contained the N241-KI mutation, and their similarity with 8 of the 9 viruses (all except 25710) at that site is not listed; likewise, all viruses have N197, which was knocked out only in the immunogen of Group 4; the similarity at residue 197 with all the others is also not listed. The glycans in the region of residues 355-360 are shifted slightly in relation to the HXB2 sequence, complicating comparisons at that site.

A Figure 5. Alignment of sequences around mutated PNGS. The amino-acid sequences of Env parental viruses BG505.T332N and B41.R315Q and nine Tier-2 viruses in the global panel (A Figure 4) were aligned. Regions comprising sequons for N-linked glycosylation that were mutated in the immunogen constructs are shown. Asn residues in PNGS:s are marked in red; HXB2-derived numbering of the Asn residues is given in bold at the top.

A Tables

A Table 1. Mutations in the BG505 immunogen trimers [a]

Group	Trimer[a]	Added mutations
1	SOSIP.v4.1 (parental)	-
2	SOSIP.v4.1 + N241-KI	S241N
3	SOSIP.v4.1 + N241-KI + N130-KI	S241N + Q130N
4	SOSIP.v4.1 + N241-KI + N197-KO	S241N + N197D
5	SOSIP.v4.1 + N241-KI + N234-KO	S241N + N234S
6	SOSIP.v4.1 + N241-KI + N276-KO	S241N + T278A
7	SOSIP.v4.1 + N241-KI + N332-KO	S241N + N332T
8	SOSIP.v4.1 + N241-KI + N355-KO	S241N + N355D + N356K

[a] All trimers were based on the BG505.T332N parental genotype. They contained the standard SOS and I559P amino-acid substitutions of the SOSIP.664 trimer design (15) plus the E64K and A316W changes that create the further-stabilized SOSIP.v4.1 version (27).

A Table 2. Mutations in the B41 immunogen trimers [a]

Group	Trimer[b]	Added mutations
9	SOSIP.v4.1 (parental)	-
10	SOSIP.v4.1 + N289-KI	A291S
11	SOSIP.v4.1 + N289-KI + N332-KO	A291S + N332T + I333L + S334N [b]
12	SOSIP.v4.1 + N289-KI + N356-KO	A291S + N356D

[a] All trimers were based on the B41.R315Q parental genotype (13). They contained the standard SOS and I559P amino-acid substitutions of the SOSIP.664 trimer design (15) plus the E64K and A316W changes that create the further-stabilized SOSIP.v4.1 version (27).

[b] The substitutions at the third and second position in the sequon are based on frequent natural amino-acid residues there (69).

A Table 3. Mutations in BG505.T332N Env-pseudoviruses [a]

Position	Mutation	Glycan	Relative dilution factor [b]
-	Parental (BG505.T332N)		1.0
130	Q130N	N130-KI	0.50
130, 241	S241N + Q130N	N130-KI, N241-KI	0.25
197	N197A	N197-KO	0.050
234	N234S	N234-KO	0.20
234, 241	S241N + N234S	N234-KO, N241-KI	1.8
241	S241N	N241-KI	0.10
241, 278	S241N + T278A	N241-KI, N276-KO	0.50
241, 291	S241N + P291T	N241-KI, N289-KI	0.30
241, 332	S241N + N332T	N241-KI, N332-KO	0.30
241, 355, 356	S241N + NN355DK	N241-KI, N355-KO	0.10
278	T278A	N276-KO	0.60
332	N332T	N332-KO	3.4
355	NN355DK	N355-KO	0.50
358, 360	I358T [c] + R360I	N356-KI [c]	0.45
465	T465N	N465-KI	1.4

[a] Other than the T332N change, the mutations used to create the parental BG505 SOSIP.v4.1 trimers (SOS, I559P and the v4.1 mutations E64K and A316W (13, 15, 27)) were not made in the corresponding BG505 pseudoviruses.

[b] The pseudoviruses were diluted to give infectivities corresponding to luminescence values of ~$2 \cdot 10^6$ (RLU) in the Tzm-bl assay. The dilution factors yielding such signals are relativized to that of the parental virus.

[c] This mutation adds a sequon adjacently to the N355 one; what glycan occupancy results on the two Asn residues is uncertain.

872

873 **A Table 4. Mutations in B41.R315Q Env-pseudoviruses [a]**

Position	Mutation	Glycan [a]	Relative dilution Factor [b]
-	Parental (B41.R315Q)		1.0
230	S230N	N230-KI	1.1
289	A291S	N289-KI	0.75
332, 333, 334	N332T + I333L + S334N	N332-KO	1.1
356	N356D	N356-KO	1.0
289, 332, 333, 334	A291S + N332T + I333L + S334N	N289-KI, N332-KO	1.3
289, 356	A291S + R315Q + N356D	N289-KI, N356-KO	0.75

874

875 [a] Other than the R315Q change, the mutations used to create the parental B41 SOSIP.v4.1
876 trimers (SOS, I559P and the v4.1 mutations E64K and A316W (13, 15, 27)) were not made in
877 the corresponding B41 pseudoviruses.

878 [b] The pseudoviruses were diluted to give infectivities corresponding to luminescence values of
879 ~2 ·10^6 (RLU) in the Tzm-bl assay. The dilution factors yielding such signals are relativized to
880 that of the parental virus.

881

882

References

1. Escolano A, Dosenovic P, Nussenzweig MC. 2017. Progress toward active or passive HIV-1 vaccination. J Exp Med 214:3-16.
2. Sanders RW, Moore JP. 2017. Native-like Env trimers as a platform for HIV-1 vaccine design. Immunol Rev 275:161-182.
3. Ward AB, Wilson IA. 2017. The HIV-1 envelope glycoprotein structure: nailing down a moving target. Immunol Rev 275:21-32.
4. Bonsignori M, Liao HX, Gao F, Williams WB, Alam SM, Montefiori DC, Haynes BF. 2017. Antibody-virus co-evolution in HIV infection: paths for HIV vaccine development. Immunol Rev 275:145-160.
5. Klein F, Mouquet H, Dosenovic P, Scheid JF, Scharf L, Nussenzweig MC. 2013. Antibodies in HIV-1 vaccine development and therapy. Science 341:1199-204.
6. Kwong PD, Mascola JR. 2018. HIV-1 vaccines based on antibody identification, B cell ontogeny, and epitope structure. Immunity 48:855-871.
7. Klasse PJ, Sanders RW, Cerutti A, Moore JP. 2012. How can HIV-type-1-Env immunogenicity be improved to facilitate antibody-based vaccine development? AIDS Res Hum Retroviruses 28:1-15.
8. Pancera M, Changela A, Kwong PD. 2017. How HIV-1 entry mechanism and broadly neutralizing antibodies guide structure-based vaccine design. Curr Opin HIV AIDS 12:229-240.
9. Cheng C, Pancera M, Bossert A, Schmidt SD, Chen RE, Chen X, Druz A, Narpala S, Doria-Rose NA, McDermott AB, Kwong PD, Mascola JR. 2015. Immunogenicity of a prefusion HIV-1 envelope trimer in complex with a quaternary-structure-specific antibody. J Virol 90:2740-55.
10. Huang J, Kang BH, Pancera M, Lee JH, Tong T, Feng Y, Imamichi H, Georgiev IS, Chuang GY, Druz A, Doria-Rose NA, Laub L, Sliepen K, van Gils MJ, de la Pena AT, Derking R, Klasse PJ, Migueles SA, Bailer RT, Alam M, Pugach P, Haynes BF, Wyatt RT, Sanders RW, Binley JM, Ward AB, Mascola JR, Kwong PD, Connors M. 2014. Broad and potent HIV-1 neutralization by a human antibody that binds the gp41-gp120 interface. Nature 515:138-42.
11. Joyce MG, Georgiev IS, Yang Y, Druz A, Geng H, Chuang GY, Kwon YD, Pancera M, Rawi R, Sastry M, Stewart-Jones GBE, Zheng A, Zhou T, Choe M, Van Galen JG, Chen RE, Lees CR, Narpala S, Chambers M, Tsybovsky Y, Baxa U, McDermott AB, Mascola JR, Kwong PD. 2017. Soluble Prefusion Closed DS-SOSIP.664-Env Trimers of Diverse HIV-1 Strains. Cell Rep 21:2992-3002.
12. Julien JP, Lee JH, Ozorowski G, Hua Y, Torrents de la Pena A, de Taeye SW, Nieusma T, Cupo A, Yasmeen A, Golabek M, Pugach P, Klasse PJ, Moore JP, Sanders RW, Ward AB, Wilson IA. 2015. Design and structure of two HIV-1 clade C SOSIP.664 trimers that increase the arsenal of native-like Env immunogens. Proc Natl Acad Sci U S A 112:11947-52.
13. Pugach P, Ozorowski G, Cupo A, Ringe R, Yasmeen A, de Val N, Derking R, Kim HJ, Korzun J, Golabek M, de Los Reyes K, Ketas TJ, Julien JP, Burton DR, Wilson IA, Sanders RW, Klasse PJ, Ward AB, Moore JP. 2015. A native-like SOSIP.664 trimer based on an HIV-1 subtype B env gene. J Virol 89:3380-95.
14. Sanders RW, van Gils MJ, Derking R, Sok D, Ketas TJ, Burger JA, Ozorowski G, Cupo A, Simonich C, Goo L, Arendt H, Kim HJ, Lee JH, Pugach P, Williams M, Debnath G,

Moldt B, van Breemen MJ, Isik G, Medina-Ramirez M, Back JW, Koff WC, Julien JP, Rakasz EG, Seaman MS, Guttman M, Lee KK, Klasse PJ, LaBranche C, Schief WR, Wilson IA, Overbaugh J, Burton DR, Ward AB, Montefiori DC, Dean H, Moore JP. 2015. HIV-1 VACCINES. HIV-1 neutralizing antibodies induced by native-like envelope trimers. Science 349:aac4223.

15. Sanders RW, Derking R, Cupo A, Julien JP, Yasmeen A, de Val N, Kim HJ, Blattner C, de la Pena AT, Korzun J, Golabek M, de Los Reyes K, Ketas TJ, van Gils MJ, King CR, Wilson IA, Ward AB, Klasse PJ, Moore JP. 2013. A next-generation cleaved, soluble HIV-1 Env trimer, BG505 SOSIP.664 gp140, expresses multiple epitopes for broadly neutralizing but not non-neutralizing antibodies. PLoS Pathog 9:e1003618.
16. Julien JP, Cupo A, Sok D, Stanfield RL, Lyumkis D, Deller MC, Klasse PJ, Burton DR, Sanders RW, Moore JP, Ward AB, Wilson IA. 2013. Crystal structure of a soluble cleaved HIV-1 envelope trimer. Science 342:1477-83.
17. Lyumkis D, Julien JP, de Val N, Cupo A, Potter CS, Klasse PJ, Burton DR, Sanders RW, Moore JP, Carragher B, Wilson IA, Ward AB. 2013. Cryo-EM structure of a fully glycosylated soluble cleaved HIV-1 envelope trimer. Science 342:1484-90.
18. Pancera M, Zhou T, Druz A, Georgiev IS, Soto C, Gorman J, Huang J, Acharya P, Chuang GY, Ofek G, Stewart-Jones GB, Stuckey J, Bailer RT, Joyce MG, Louder MK, Tumba N, Yang Y, Zhang B, Cohen MS, Haynes BF, Mascola JR, Morris L, Munro JB, Blanchard SC, Mothes W, Connors M, Kwong PD. 2014. Structure and immune recognition of trimeric pre-fusion HIV-1 Env. Nature 514:455-61.
19. Yasmeen A, Ringe R, Derking R, Cupo A, Julien JP, Burton DR, Ward AB, Wilson IA, Sanders RW, Moore JP, Klasse PJ. 2014. Differential binding of neutralizing and non-neutralizing antibodies to native-like soluble HIV-1 Env trimers, uncleaved Env proteins, and monomeric subunits. Retrovirology 11:41.
20. Klasse PJ. 2012. The molecular basis of HIV entry. Cell Microbiol 14:1183-92.
21. Ugolini S, Mondor I, Parren PW, Burton DR, Tilley SA, Klasse PJ, Sattentau QJ. 1997. Inhibition of virus attachment to CD4+ target cells is a major mechanism of T cell line-adapted HIV-1 neutralization. J Exp Med 186:1287-98.
22. Klasse PJ. 2014. Neutralization of virus infectivity by antibodies: old problems in new perspectives. Adv Biol 2014:1-24.
23. Parren PW, Mondor I, Naniche D, Ditzel HJ, Klasse PJ, Burton DR, Sattentau QJ. 1998. Neutralization of human immunodeficiency virus type 1 by antibody to gp120 is determined primarily by occupancy of sites on the virion irrespective of epitope specificity. J Virol 72:3512-9.
24. Ruprecht CR, Krarup A, Reynell L, Mann AM, Brandenberg OF, Berlinger L, Abela IA, Regoes RR, Gunthard HF, Rusert P, Trkola A. 2011. MPER-specific antibodies induce gp120 shedding and irreversibly neutralize HIV-1. J Exp Med 208:439-54.
25. Julien JP, Sok D, Khayat R, Lee JH, Doores KJ, Walker LM, Ramos A, Diwanji DC, Pejchal R, Cupo A, Katpally U, Depetris RS, Stanfield RL, McBride R, Marozsan AJ, Paulson JC, Sanders RW, Moore JP, Burton DR, Poignard P, Ward AB, Wilson IA. 2013. Broadly neutralizing antibody PGT121 allosterically modulates CD4 binding via recognition of the HIV-1 gp120 V3 base and multiple surrounding glycans. PLoS Pathog 9:e1003342.

26. Platt EJ, Gomes MM, Kabat D. 2012. Kinetic mechanism for HIV-1 neutralization by antibody 2G12 entails reversible glycan binding that slows cell entry. Proc Natl Acad Sci U S A 109:7829-34.
27. de Taeye SW, Ozorowski G, Torrents de la Pena A, Guttman M, Julien JP, van den Kerkhof TL, Burger JA, Pritchard LK, Pugach P, Yasmeen A, Crampton J, Hu J, Bontjer I, Torres JL, Arendt H, DeStefano J, Koff WC, Schuitemaker H, Eggink D, Berkhout B, Dean H, LaBranche C, Crotty S, Crispin M, Montefiori DC, Klasse PJ, Lee KK, Moore JP, Wilson IA, Ward AB, Sanders RW. 2015. Immunogenicity of stabilized HIV-1 envelope trimers with reduced exposure of non-neutralizing epitopes. Cell 163:1702-15.
28. Havenar-Daughton C, Carnathan DG, Torrents de la Pena A, Pauthner M, Briney B, Reiss SM, Wood JS, Kaushik K, van Gils MJ, Rosales SL, van der Woude P, Locci M, Le KM, de Taeye SW, Sok D, Mohammed AU, Huang J, Gumber S, Garcia A, Kasturi SP, Pulendran B, Moore JP, Ahmed R, Seumois G, Burton DR, Sanders RW, Silvestri G, Crotty S. 2016. Direct probing of germinal center responses reveals immunological features and bottlenecks for neutralizing antibody responses to HIV Env trimer. Cell Rep 17:2195-2209.
29. Klasse PJ, LaBranche CC, Ketas TJ, Ozorowski G, Cupo A, Pugach P, Ringe RP, Golabek M, van Gils MJ, Guttman M, Lee KK, Wilson IA, Butera ST, Ward AB, Montefiori DC, Sanders RW, Moore JP. 2016. Sequential and simultaneous immunization of rabbits with HIV-1 envelope glycoprotein SOSIP.664 trimers from Clades A, B and C. PLoS Pathog 12:e1005864.
30. Pauthner M, Havenar-Daughton C, Sok D, Nkolola JP, Bastidas R, Boopathy AV, Carnathan DG, Chandrashekar A, Cirelli KM, Cottrell CA, Eroshkin AM, Guenaga J, Kaushik K, Kulp DW, Liu J, McCoy LE, Oom AL, Ozorowski G, Post KW, Sharma SK, Steichen JM, de Taeye SW, Tokatlian T, Torrents de la Pena A, Butera ST, LaBranche CC, Montefiori DC, Silvestri G, Wilson IA, Irvine DJ, Sanders RW, Schief WR, Ward AB, Wyatt RT, Barouch DH, Crotty S, Burton DR. 2017. Elicitation of robust Tier 2 neutralizing antibody responses in nonhuman primates by HIV envelope trimer immunization using optimized approaches. Immunity 46:1073-1088 e6.
31. Berzofsky JA. 1985. Intrinsic and extrinsic factors in protein antigenic structure. Science 229:932-40.
32. Laver WG, Air GM, Webster RG, Smith-Gill SJ. 1990. Epitopes on protein antigens: misconceptions and realities. Cell 61:553-6.
33. Crispin M, Ward AB, Wilson IA. 2018. Structure and immune recognition of the HIV glycan shield. Annu Rev Biophys doi:10.1146/annurev-biophys-060414-034156.
34. Behrens AJ, Vasiljevic S, Pritchard LK, Harvey DJ, Andev RS, Krumm SA, Struwe WB, Cupo A, Kumar A, Zitzmann N, Seabright GE, Kramer HB, Spencer DI, Royle L, Lee JH, Klasse PJ, Burton DR, Wilson IA, Ward AB, Sanders RW, Moore JP, Doores KJ, Crispin M. 2016. Composition and antigenic effects of individual glycan sites of a trimeric HIV-1 envelope glycoprotein. Cell Rep 14:2695-706.
35. Behrens AJ, Harvey DJ, Milne E, Cupo A, Kumar A, Zitzmann N, Struwe WB, Moore JP, Crispin M. 2017. Molecular Architecture of the Cleavage-Dependent Mannose Patch on a Soluble HIV-1 Envelope Glycoprotein Trimer. J Virol 91.
36. Pritchard LK, Spencer DI, Royle L, Bonomelli C, Seabright GE, Behrens AJ, Kulp DW, Menis S, Krumm SA, Dunlop DC, Crispin DJ, Bowden TA, Scanlan CN, Ward AB, Schief WR, Doores KJ, Crispin M. 2015. Glycan clustering stabilizes the mannose patch

of HIV-1 and preserves vulnerability to broadly neutralizing antibodies. Nat Commun 6:7479.

37. Cao L, Diedrich JK, Kulp DW, Pauthner M, He L, Park SR, Sok D, Su CY, Delahunty CM, Menis S, Andrabi R, Guenaga J, Georgeson E, Kubitz M, Adachi Y, Burton DR, Schief WR, Yates Iii JR, Paulson JC. 2017. Global site-specific N-glycosylation analysis of HIV envelope glycoprotein. Nat Commun 8:14954.

38. Klasse PJ, Ketas TJ, Cottrell CA, Ozorowski G, Debnath G, Camara D, Francomano E, Pugach P, Ringe RP, LaBranche CC, van Gils MJ, Bricault CA, Barouch DH, Crotty S, Silvestri G, Kasturi S, Pulendran B, Wilson IA, Montefiori DC, Sanders RW, Ward AB, Moore JP. 2018. Epitopes for neutralizing antibodies induced by HIV-1 envelope glycoprotein BG505 SOSIP trimers in rabbits and macaques. PLoS Pathog 14:e1006913.

39. Zhou T, Doria-Rose NA, Cheng C, Stewart-Jones GBE, Chuang GY, Chambers M, Druz A, Geng H, McKee K, Kwon YD, O'Dell S, Sastry M, Schmidt SD, Xu K, Chen L, Chen RE, Louder MK, Pancera M, Wanninger TG, Zhang B, Zheng A, Farney SK, Foulds KE, Georgiev IS, Joyce MG, Lemmin T, Narpala S, Rawi R, Soto C, Todd JP, Shen CH, Tsybovsky Y, Yang Y, Zhao P, Haynes BF, Stamatatos L, Tiemeyer M, Wells L, Scorpio DG, Shapiro L, McDermott AB, Mascola JR, Kwong PD. 2017. Quantification of the impact of the HIV-1-glycan shield on antibody elicitation. Cell Rep 19:719-732.

40. Crooks ET, Tong T, Chakrabarti B, Narayan K, Georgiev IS, Menis S, Huang X, Kulp D, Osawa K, Muranaka J, Stewart-Jones G, Destefano J, O'Dell S, LaBranche C, Robinson JE, Montefiori DC, McKee K, Du SX, Doria-Rose N, Kwong PD, Mascola JR, Zhu P, Schief WR, Wyatt RT, Whalen RG, Binley JM. 2015. Vaccine-elicited Tier 2 HIV-1 neutralizing antibodies bind to quaternary epitopes involving glycan-deficient patches proximal to the CD4 binding site. PLoS Pathog 11:e1004932.

41. Montefiori DC, Roederer M, Morris L, Seaman MS. 2018. Neutralization tiers of HIV-1. Curr Opin HIV AIDS 13:128-136.

42. Seaman MS, Janes H, Hawkins N, Grandpre LE, Devoy C, Giri A, Coffey RT, Harris L, Wood B, Daniels MG, Bhattacharya T, Lapedes A, Polonis VR, McCutchan FE, Gilbert PB, Self SG, Korber BT, Montefiori DC, Mascola JR. 2010. Tiered categorization of a diverse panel of HIV-1 Env pseudoviruses for assessment of neutralizing antibodies. J Virol 84:1439-52.

43. Hu JK, Crampton JC, Cupo A, Ketas T, van Gils MJ, Sliepen K, de Taeye SW, Sok D, Ozorowski G, Deresa I, Stanfield R, Ward AB, Burton DR, Klasse PJ, Sanders RW, Moore JP, Crotty S. 2015. Murine antibody responses to cleaved soluble HIV-1 envelope trimers are highly restricted in specificity. J Virol 89:10383-98.

44. Kulp DW, Steichen JM, Pauthner M, Hu X, Schiffner T, Liguori A, Cottrell CA, Havenar-Daughton C, Ozorowski G, Georgeson E, Kalyuzhniy O, Willis JR, Kubitz M, Adachi Y, Reiss SM, Shin M, de Val N, Ward AB, Crotty S, Burton DR, Schief WR. 2017. Structure-based design of native-like HIV-1 envelope trimers to silence non-neutralizing epitopes and eliminate CD4 binding. Nat Commun 8:1655.

45. Moore JP. 2017. Kulp, D. W. et al. Structure-based design of native-like HIV-1 envelope trimers to silence non-neutralizing epitopes and eliminate CD4 binding. . Nat Commun 8:https://www.nature.com/articles/s41467-017-01549-6.

46. Medina-Ramirez M, Sanders RW, Klasse PJ. 2014. Targeting B-cell germlines and focusing affinity maturation: the next hurdles in HIV-1-vaccine development? Expert Rev Vaccines 13:449-52.

47. Stamatatos L, Pancera M, McGuire AT. 2017. Germline-targeting immunogens. Immunol Rev 275:203-216.
48. Medina-Ramirez M, Garces F, Escolano A, Skog P, de Taeye SW, Del Moral-Sanchez I, McGuire AT, Yasmeen A, Behrens AJ, Ozorowski G, van den Kerkhof T, Freund NT, Dosenovic P, Hua Y, Gitlin AD, Cupo A, van der Woude P, Golabek M, Sliepen K, Blane T, Kootstra N, van Breemen MJ, Pritchard LK, Stanfield RL, Crispin M, Ward AB, Stamatatos L, Klasse PJ, Moore JP, Nemazee D, Nussenzweig MC, Wilson IA, Sanders RW. 2017. Design and crystal structure of a native-like HIV-1 envelope trimer that engages multiple broadly neutralizing antibody precursors in vivo. J Exp Med doi:10.1084/jem.20161160.
49. Chuang GY, Geng H, Pancera M, Xu K, Cheng C, Acharya P, Chambers M, Druz A, Tsybovsky Y, Wanninger TG, Yang Y, Doria-Rose NA, Georgiev IS, Gorman J, Joyce MG, O'Dell S, Zhou T, McDermott AB, Mascola JR, Kwong PD. 2017. Structure-based design of a soluble prefusion-closed HIV-1 Env trimer with reduced CD4 affinity and improved immunogenicity. J Virol 91.
50. Torrents de la Pena A, Julien JP, de Taeye SW, Garces F, Guttman M, Ozorowski G, Pritchard LK, Behrens AJ, Go EP, Burger JA, Schermer EE, Sliepen K, Ketas TJ, Pugach P, Yasmeen A, Cottrell CA, Torres JL, Vavourakis CD, van Gils MJ, LaBranche C, Montefiori DC, Desaire H, Crispin M, Klasse PJ, Lee KK, Moore JP, Ward AB, Wilson IA, Sanders RW. 2017. Improving the immunogenicity of native-like HIV-1 envelope trimers by hyperstabilization. Cell Rep 20:1805-1817.
51. Ringe RP, Ozorowski G, Rantalainen K, Struwe WB, Matthews K, Torres JL, Yasmeen A, Cottrell CA, Ketas TJ, LaBranche CC, Montefiori DC, Cupo A, Crispin M, Wilson IA, Ward AB, Sanders RW, Klasse PJ, Moore JP. 2017. Reducing V3 antigenicity and immunogenicity on soluble, native-like HIV-1 Env SOSIP trimers. J Virol 91.
52. Behrens AJ, Kumar A, Medina-Ramirez M, Cupo A, Marshall K, Cruz Portillo VM, Harvey DJ, Ozorowski G, Zitzmann N, Wilson IA, Ward AB, Struwe WB, Moore JP, Sanders RW, Crispin M. 2018. Integrity of Glycosylation Processing of a Glycan-Depleted Trimeric HIV-1 Immunogen Targeting Key B-Cell Lineages. J Proteome Res 17:987-999.
53. Wagh K, Kreider EF, Li Y, Barbian HJ, Learn GH, Giorgi E, Hraber PT, Decker TG, Smith AG, Gondim MV, Gillis L, Wandzilak J, Chuang GY, Rawi R, Cai F, Pellegrino P, Williams I, Overbaugh J, Gao F, Kwong PD, Haynes BF, Shaw GM, Borrow P, Seaman MS, Hahn BH, Korber B. 2018. Completeness of HIV-1 envelope glycan shield at transmission determines neutralization breadth. Cell Rep 25:893-908 e7.
54. Torrents de la Pena A, de Taeye SW, Sliepen K, LaBranche CC, Burger JA, Schermer EE, Montefiori DC, Moore JP, Klasse PJ, Sanders RW. 2018. Immunogenicity in rabbits of HIV-1 SOSIP trimers from Clades A, B, and C, given individually, sequentially, or in combination. J Virol 92.
55. Dubrovskaya V, Guenaga J, de Val N, Wilson R, Feng Y, Movsesyan A, Karlsson Hedestam GB, Ward AB, Wyatt RT. 2017. Targeted N-glycan deletion at the receptor-binding site retains HIV Env NFL trimer integrity and accelerates the elicited antibody response. PLoS Pathog 13:e1006614.
56. Huang J, Kang BH, Ishida E, Zhou T, Griesman T, Sheng Z, Wu F, Doria-Rose NA, Zhang B, McKee K, O'Dell S, Chuang GY, Druz A, Georgiev IS, Schramm CA, Zheng A, Joyce MG, Asokan M, Ransier A, Darko S, Migueles SA, Bailer RT, Louder MK,

Alam SM, Parks R, Kelsoe G, Von Holle T, Haynes BF, Douek DC, Hirsch V, Seaman MS, Shapiro L, Mascola JR, Kwong PD, Connors M. 2016. Identification of a CD4-binding-site antibody to HIV that evolved near-pan neutralization breadth. Immunity 45:1108-1121.

57. Rantalainen K, Berndsen ZT, Murrell S, Cao L, Omorodion O, Torres JL, Wu M, Umotoy J, Copps J, Poignard P, Landais E, Paulson JC, Wilson IA, Ward AB. 2018. Co-evolution of HIV Envelope and Apex-Targeting Neutralizing Antibody Lineage Provides Benchmarks for Vaccine Design. Cell Rep 23:3249-3261.
58. Struwe WB, Stuckmann A, Behrens AJ, Pagel K, Crispin M. 2017. Global N-Glycan Site Occupancy of HIV-1 gp120 by Metabolic Engineering and High-Resolution Intact Mass Spectrometry. ACS Chem Biol 12:357-361.
59. Klasse PJ. 2007. Modeling how many envelope glycoprotein trimers per virion participate in human immunodeficiency virus infectivity and its neutralization by antibody. Virology 369:245-62.
60. Klasse PJ, Moore JP. 1996. Quantitative model of antibody- and soluble CD4-mediated neutralization of primary isolates and T-cell line-adapted strains of human immunodeficiency virus type 1. J Virol 70:3668-77.
61. deCamp A, Hraber P, Bailer RT, Seaman MS, Ochsenbauer C, Kappes J, Gottardo R, Edlefsen P, Self S, Tang H, Greene K, Gao H, Daniell X, Sarzotti-Kelsoe M, Gorny MK, Zolla-Pazner S, LaBranche CC, Mascola JR, Korber BT, Montefiori DC. 2014. Global panel of HIV-1 Env reference strains for standardized assessments of vaccine-elicited neutralizing antibodies. J Virol 88:2489-507.
62. Julien JP, Lee JH, Cupo A, Murin CD, Derking R, Hoffenberg S, Caulfield MJ, King CR, Marozsan AJ, Klasse PJ, Sanders RW, Moore JP, Wilson IA, Ward AB. 2013. Asymmetric recognition of the HIV-1 trimer by broadly neutralizing antibody PG9. Proc Natl Acad Sci U S A 110:4351-6.
63. Sastry M, Zhang B, Chen M, Joyce MG, Kong WP, Chuang GY, Ko K, Kumar A, Silacci C, Thom M, Salazar AM, Corti D, Lanzavecchia A, Taylor G, Mascola JR, Graham BS, Kwong PD. 2017. Adjuvants and the vaccine response to the DS-Cav1-stabilized fusion glycoprotein of respiratory syncytial virus. PLoS One 12:e0186854.
64. Wegmann F, Moghaddam AE, Schiffner T, Gartlan KH, Powell TJ, Russell RA, Baart M, Carrow EW, Sattentau QJ. 2015. The carbomer-lecithin adjuvant adjuplex has potent immunoactivating properties and elicits protective adaptive immunity against influenza virus challenge in mice. Clin Vaccine Immunol 22:1004-12.
65. Xu K, Acharya P, Kong R, Cheng C, Chuang GY, Liu K, Louder MK, O'Dell S, Rawi R, Sastry M, Shen CH, Zhang B, Zhou T, Asokan M, Bailer RT, Chambers M, Chen X, Choi CW, Dandey VP, Doria-Rose NA, Druz A, Eng ET, Farney SK, Foulds KE, Geng H, Georgiev IS, Gorman J, Hill KR, Jafari AJ, Kwon YD, Lai YT, Lemmin T, McKee K, Ohr TY, Ou L, Peng D, Rowshan AP, Sheng Z, Todd JP, Tsybovsky Y, Viox EG, Wang Y, Wei H, Yang Y, Zhou AF, Chen R, Yang L, Scorpio DG, McDermott AB, Shapiro L, et al. 2018. Epitope-based vaccine design yields fusion peptide-directed antibodies that neutralize diverse strains of HIV-1. Nat Med 24:857-867.
66. Lee JH, Andrabi R, Su CY, Yasmeen A, Julien JP, Kong L, Wu NC, McBride R, Sok D, Pauthner M, Cottrell CA, Nieusma T, Blattner C, Paulson JC, Klasse PJ, Wilson IA, Burton DR, Ward AB. 2017. A broadly neutralizing antibody targets the dynamic HIV

envelope trimer apex via a long, rigidified, and anionic beta-hairpin structure. Immunity 46:690-702.
67. Lee JH, Ozorowski G, Ward AB. 2016. Cryo-EM structure of a native, fully glycosylated, cleaved HIV-1 envelope trimer. Science 351:1043-8.
68. Pettersen EF, Goddard TD, Huang CC, Couch GS, Greenblatt DM, Meng EC, Ferrin TE. 2004. UCSF Chimera--a visualization system for exploratory research and analysis. J Comput Chem 25:1605-12.
69. LANL. https://www.hiv.lanl.gov/content/sequence/HIV/mainpage.html.

A

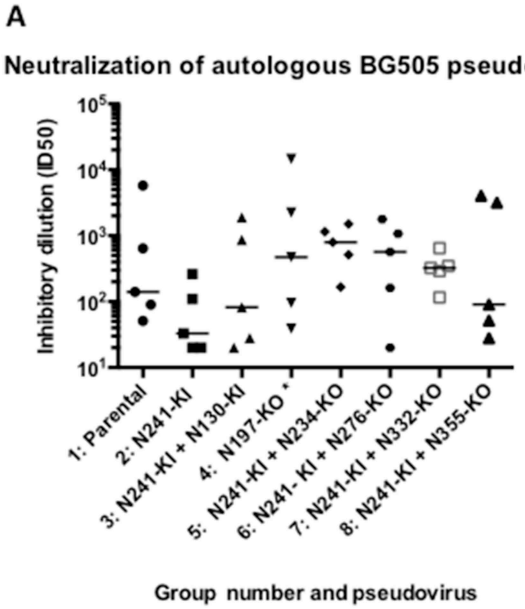
Neutralization of autologous BG505 pseudoviruses
Inhibitory dilution (ID50)
10^5
10^4
10^3
10^2
10^1
1: Parental
2: N241-KI
3: N241-KI + N130-KI
4: N197-KO *
5: N241-KI + N234-KO
6: N241- KI + N276-KO
7: N241-KI + N332-KO
8: N241-KI + N355-KO
Group number and pseudovirus

B

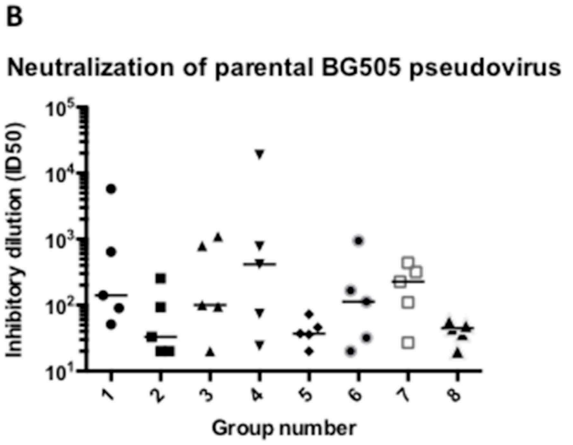
Neutralization of parental BG505 pseudovirus
Inhibitory dilution (ID50)
10^5
10^4
10^3
10^2
10^1
1
2
3
4
5
6
7
8
Group number

A

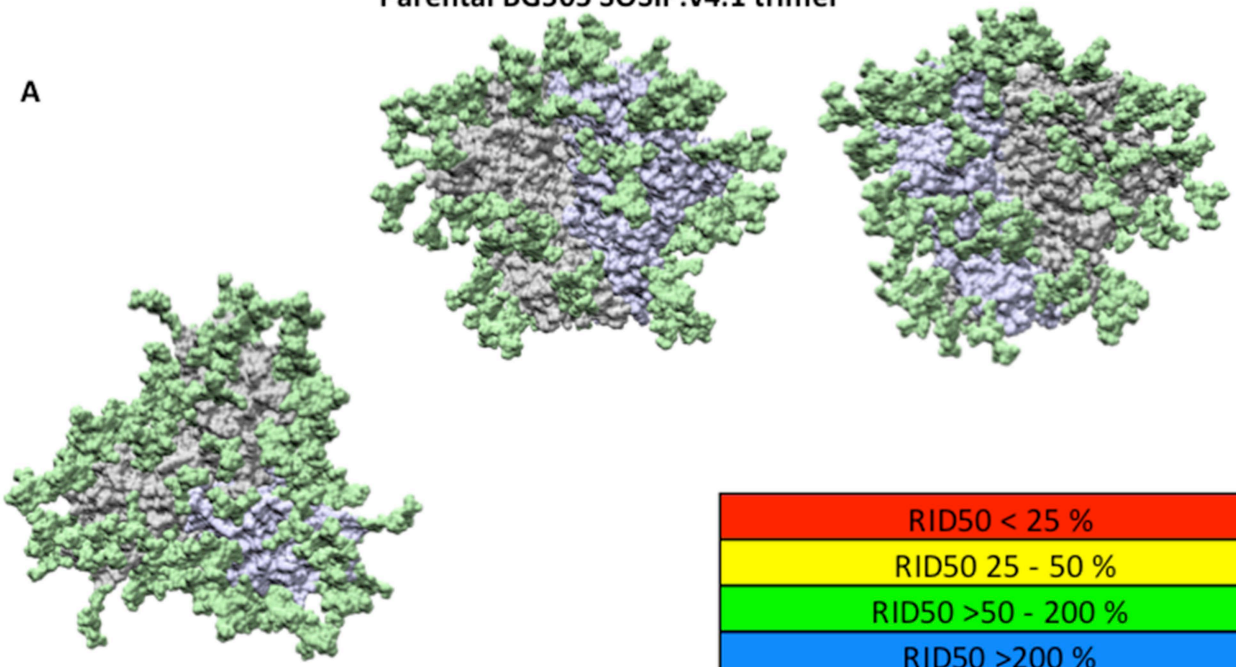

B

Group 1	ID50	RID50 (Mutant/Parental) %				
Rabbit	Parental	Parental	N241-KI	N241-KI + N289-KI	N356-KI + R360I	N465-KI
r2213-1	5800	100	32	28	160	110
r2214-1	640	100	5	6	180	130

BG505 SOSIP.v4.1-N241-KI trimer

A

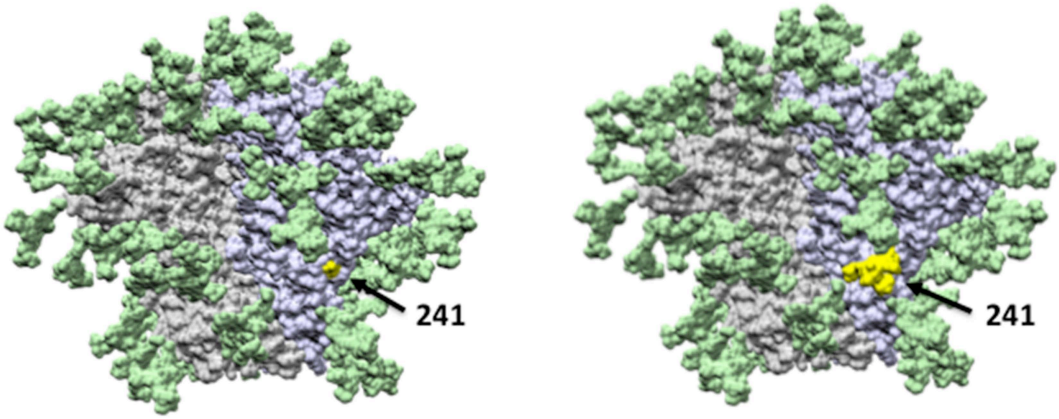

B

Group 2	ID50	RID50 (Mutant/Parental) %				
Rabbit	Parental	Parental	N241-KI	N241-KI + N289-KI	N356-KI R360I	N465-KI
r2220-2	250	100	100	89	34	57

BG505 SOSIP.v4.1-N241-KI + N130-KI trimer

A

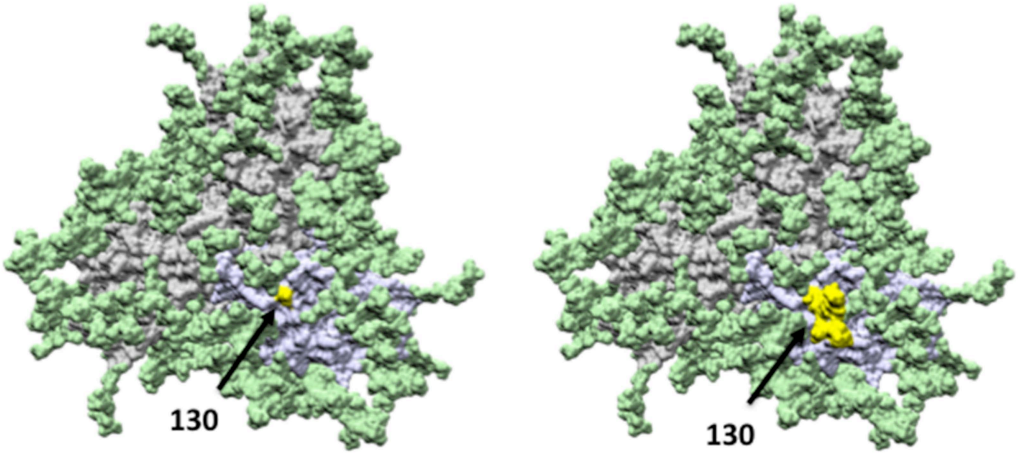

B

Group 3	ID50	RID50 (Mutant/Parental) %						
Rabbit	Parental	Parental	N130-KI	N130-KI + N241-KI	N241-KI	N241-KI + N289-KI	N356-KI + R360I	N465-KI
r2224-3	1100	100	150	170	95	130	81	71
r2225-3	930	100	82	110	100	61	3	3

BG505 SOSIP.v4.1-N241-KI + N197-KO trimer

A

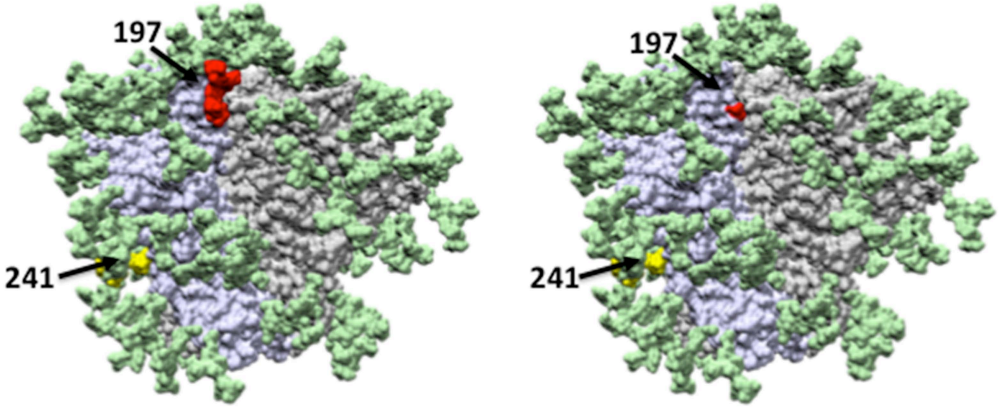

B

Group 4	ID50	RID50 (Mutant/Parental) %					
Rabbit	Parental	Parental	N197-KO	N241-KI	N241-KI + N289-KI	N356-KI + R360I	N465-KI
r2228-4	19000	100	78	140	77	16	34
r2229-4	770	100	290	110	95	110	110
r2231-4	420	100	110	220	64	13	50

BG505 SOSIP.v4.1-N241-KI + N234-KO trimer

A

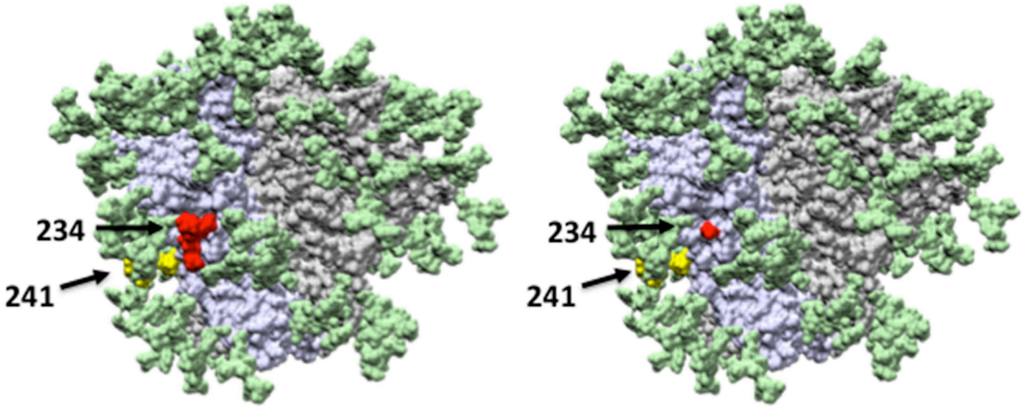

B

Group 5	ID50	RID50 (Mutant/Parental) %		
Rabbit	Parental	Parental	N234-KO	N234-KO + N241-KI
r2232-5	73	100	1100	1100
r2233-5	20	100	700	840
r2234-5	46	100	830	1100
r2235-5	37	100	3800	4100
r2236-5	36	100	3700	3200

BG505 SOSIP.v4.1-N241-KI + N276-KO trimer

A

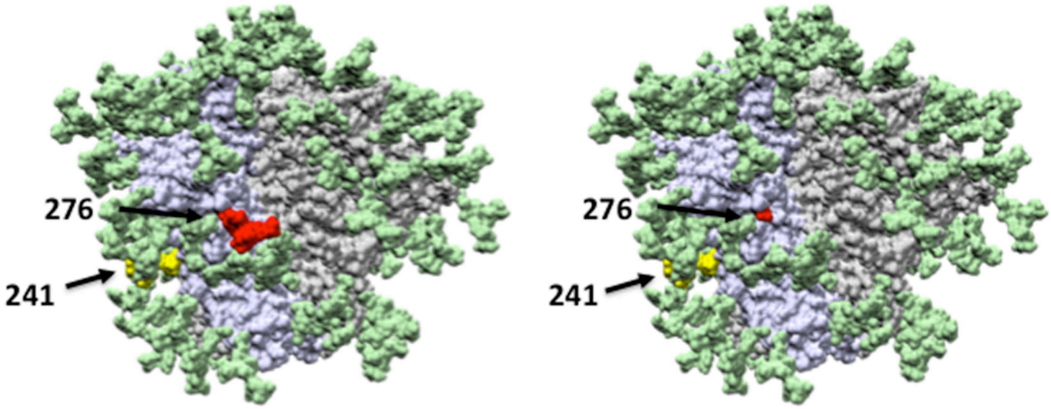

B

Group 6	ID50	RID50 (Mutant/Parental) %						
Rabbit	Parental	Parental	N276-KO	N276-KO + N241-KI	N241-KI	N241-KI + N289-KI	N356-KI + R360I	N465-KI
r2237-6	940	100	55	60	58	49	10	14
r2238-6	32	100	6400	5600				
r2240-6	110	100	1200	950	63	66	79	98
r2241-6	170	100	104	97	114	82	45	45

BG505 SOSIP.v4.1-N241-KI + N332-KO trimer

A

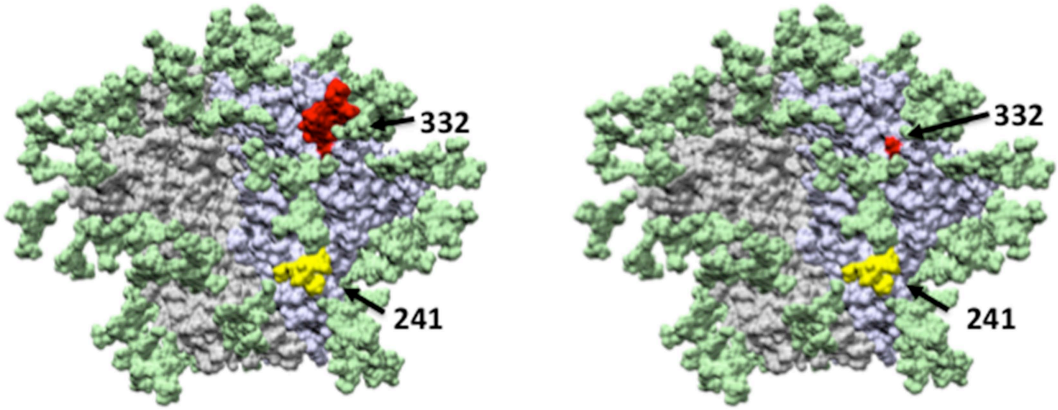

B

Group 7	ID50	RID50 (Mutant/Parental) %						
Rabbit	Parental	Parental	N332-KO	N332-KO + N241-KI	N241-KI	N241-KI + N289-KI	N356-KI + R360I	N465-KI
r2242-7	230	100	140	150	75	59	23	24
r2243-7	27	100	1500	1100				
r2244-7	440	100	71	75	82	65	4	7
r2245-7	150	100	76	105	75	39	21	14
r2246-7	320	100	220	200	93	35	19	19

BG505 SOSIP.v4.1-N241-KI + N355-KO trimer

A

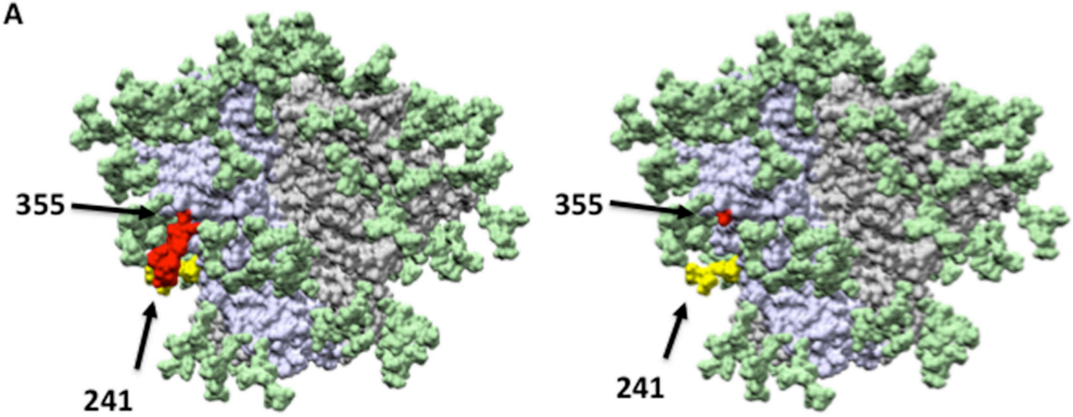

B

Group 8	ID50	RID50 (Mutant/Parental) %		
Rabbit	Parental	Parental	N355-KO	N355-KO + N241-KI
r2248-8	37	100	25000	11000
r2249-8	20	100	620	460
r2250-8	57	100	19000	5600

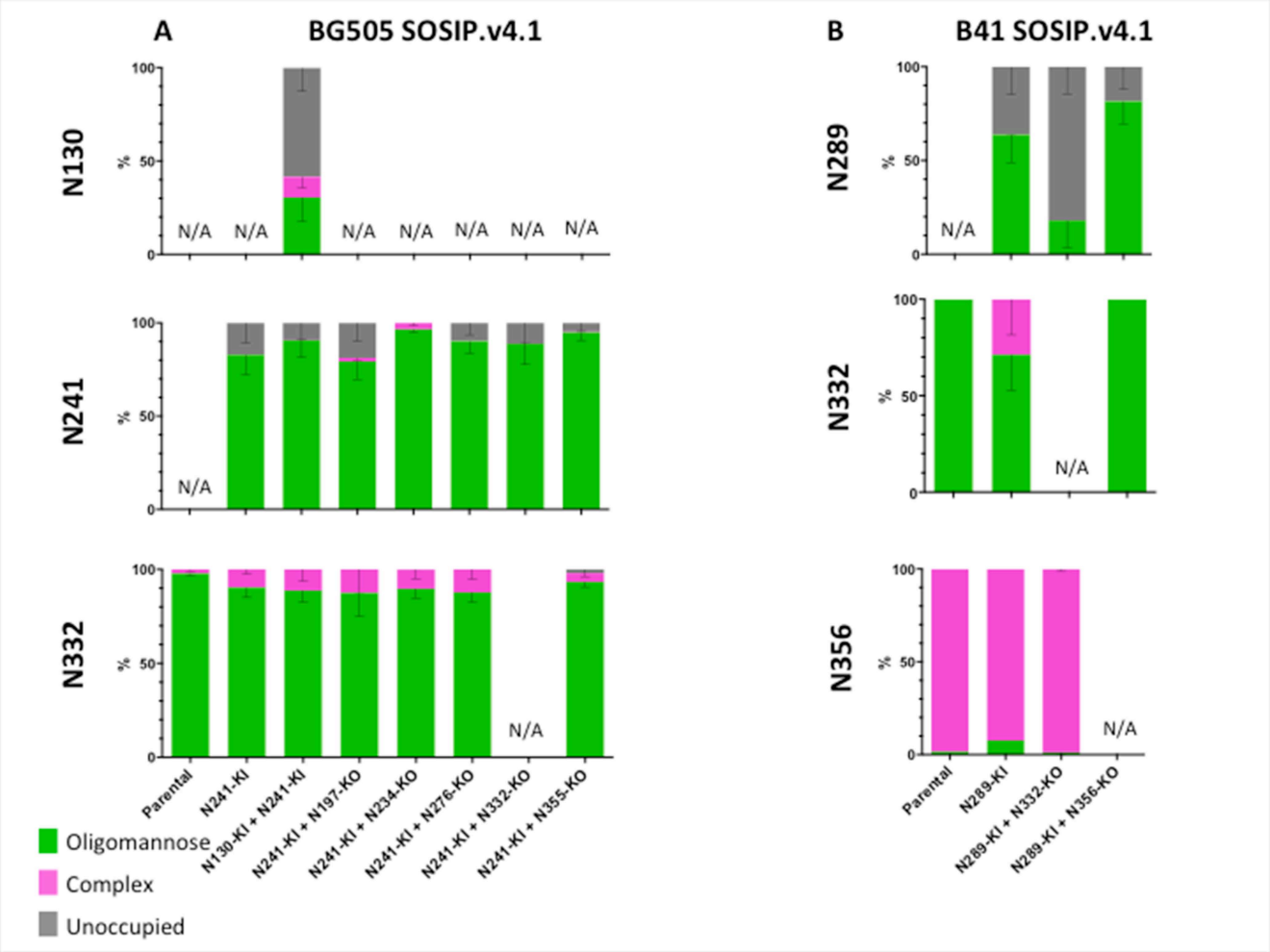
A
BG505 SOSIP.v4.1
B
B41 SOSIP.v4.1
N130
N241
N332
N289
N332
N356
%
100
50
0
N/A
Parental
N241-KI
N130-KI + N241-KI
N241-KI + N197-KO
N241-KI + N234-KO
N241-KI + N276-KO
N241-KI + N332-KO
N241-KI + N355-KO
N289-KI
N289-KI + N332-KO
N289-KI + N356-KO
Oligomannose
Complex
Unoccupied

A

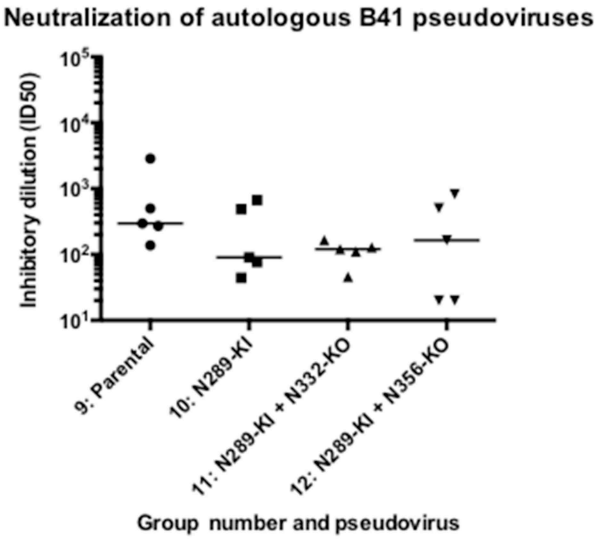
Neutralization of autologous B41 pseudoviruses
Inhibitory dilution (ID50)
10^5
10^4
10^3
10^2
10^1
9: Parental
10: N289-KI
11: N289-KI + N332-KO
12: N289-KI + N356-KO
Group number and pseudovirus

B

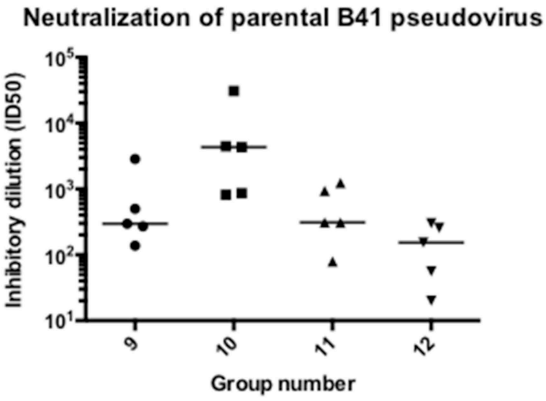
Neutralization of parental B41 pseudovirus
Inhibitory dilution (ID50)
10^5
10^4
10^3
10^2
10^1
9
10
11
12
Group number

Parental B41 SOSIP.v4.1 trimer

A

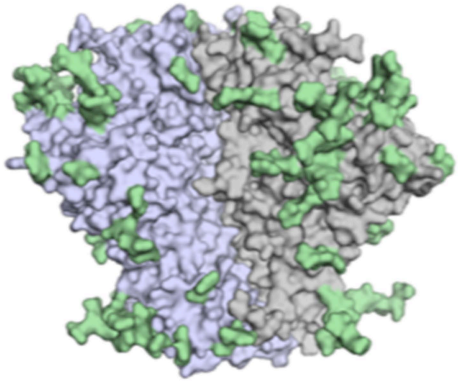

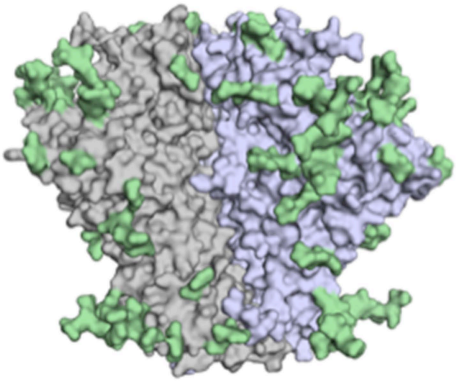

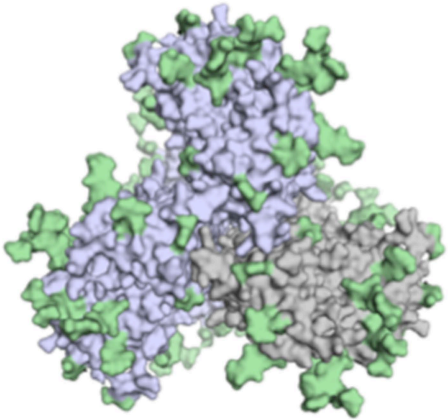

B

Group 9	ID50	RID50 (Mutant/Parental) %		
Rabbit	Parental	Parental	N289-KI	N230-KI
r2257-9	270	100	30	23
r2258-9	297	100	26	20
r2259-9	500	100	17	9
r2260-9	2859	100	32	32

A

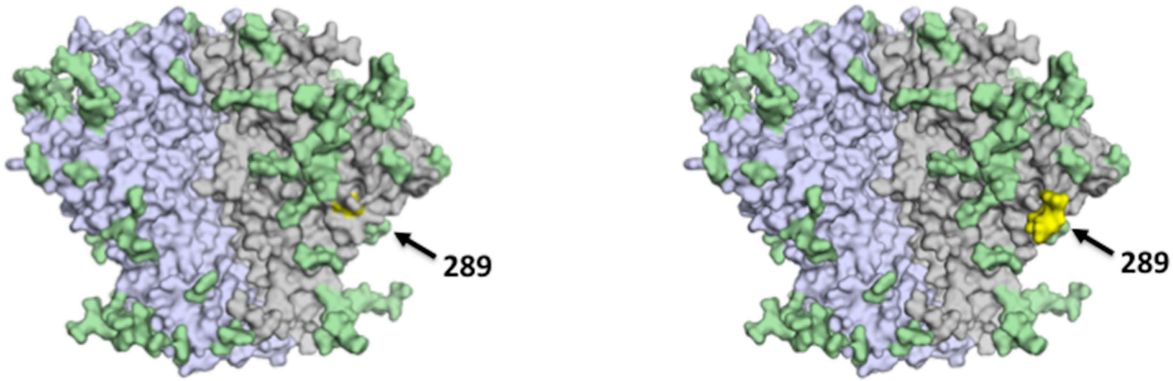

B

Group 10	ID50	RID50 (Mutant/Parental) %		
Rabbit	Parental	Parental	N289-KI	N230-KI
r2261-10	4451	100	11	23
r2262-10	819	100	9	2
r2263-10	30828	100	2	0
r2264-10	4327	100	2	0
r2265-10	862	100	5	52

B41 SOSIP.v4.1-N289-KI + N332-KO trimer

A

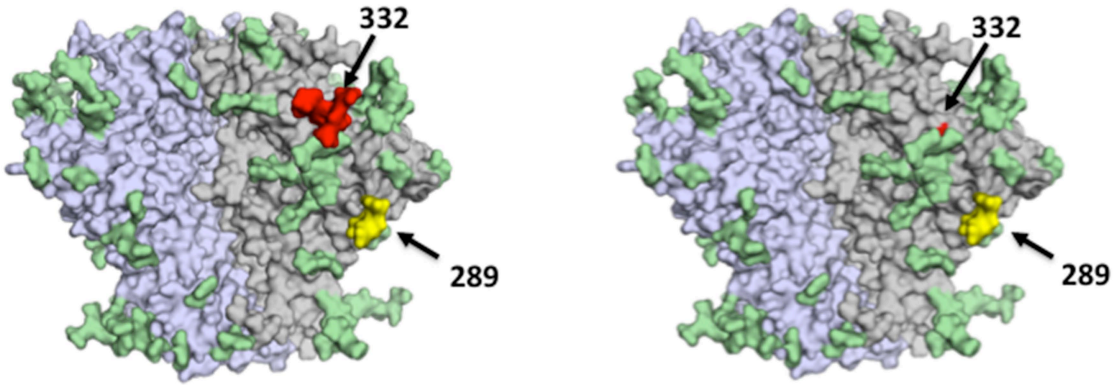

B

Group 11	ID50	RID50 (Mutant/Parental) %				
Rabbit	Parental	Parental	N332-KO	N332-KO + N289-KI	N289-KI	N230-KI
r2267-11	935	100	99	14	14	34
r2268-11	307	100	93	36	26	32
r2269-11	310	100	73	53	21	37
r2270-11	1238	100	79	10	11	26

B41 SOSIP.v4.1-N289-KI + N356-KO trimer

A

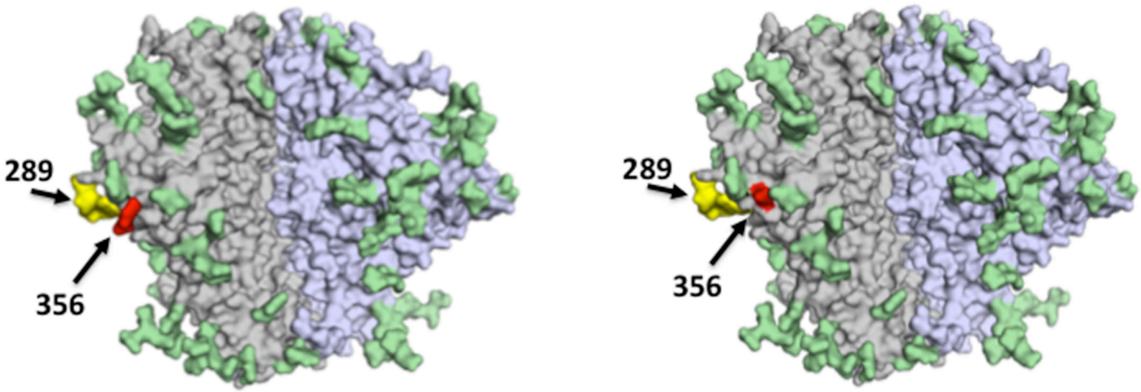

B

Group 12	ID50	RID50 (Mutant/Parental) %				
Rabbit	Parental	Parental	N356-KO	N356-KO + N289-KI	N289-KI	N230-KI
r2271-12	153	100	230	13	13	25
r2272-12	56	100	3800	900		
r2273-12	256	100	610	320	67	48
r2275-12	300	100	83	55	7	10

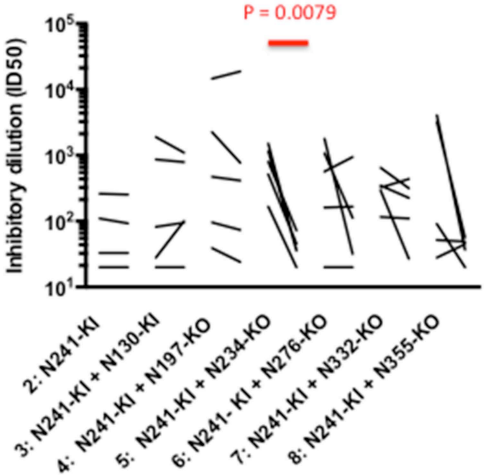
P = 0.0079
Inhibitory dilution (ID50)
10^5
10^4
10^3
10^2
10^1
2: N241-KI
3: N241-KI + N130-KI
4: N241-KI + N197-KO
5: N241-KI + N234-KO
6: N241- KI + N276-KO
7: N241-KI + N332-KO
8: N241-KI + N355-KO

A

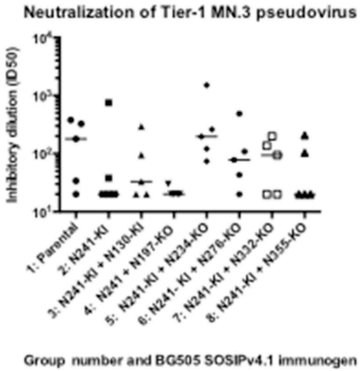
Neutralization of Tier-1 MN.3 pseudovirus
Inhibitory dilution (ID50)
1: Parental
2: N241-KI
3: N241-KI + N130-KI
4: N241 + N197-KO
5: N241-KI + N234-KO
6: N241- KI + N276-KO
7: N241-KI + N332-KO
8: N241-KI + N355-KO
Group number and BG505 SOSIPv4.1 immunogen

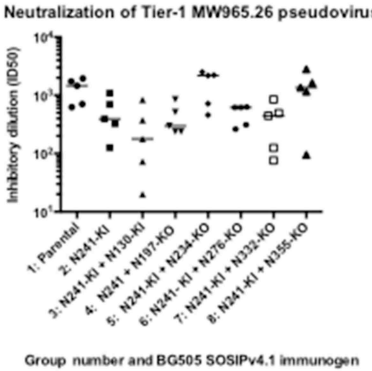
Neutralization of Tier-1 MW965.26 pseudovirus
Inhibitory dilution (ID50)
1: Parental
2: N241-KI
3: N241-KI + N130-KI
4: N241 + N197-KO
5: N241-KI + N234-KO
6: N241- KI + N276-KO
7: N241-KI + N332-KO
8: N241-KI + N355-KO
Group number and BG505 SOSIPv4.1 immunogen

B

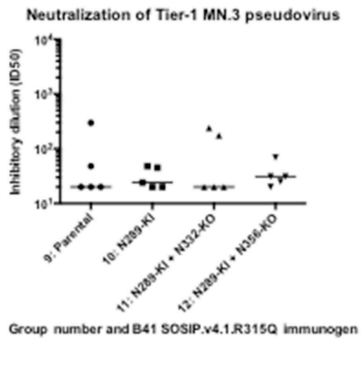
Neutralization of Tier-1 MN.3 pseudovirus
Inhibitory dilution (ID50)
9: Parental
10: N289-KI
11: N289-KI + N332-KO
12: N289-KI + N356-KO
Group number and B41 SOSIP.v4.1.R315Q immunogen

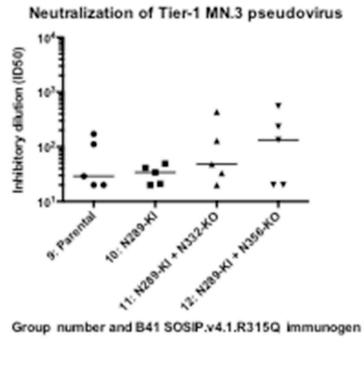
Neutralization of Tier-1 MN.3 pseudovirus
Inhibitory dilution (ID50)
9: Parental
10: N289-KI
11: N289-KI + N332-KO
12: N289-KI + N356-KO
Group number and B41 SOSIP.v4.1.R315Q immunogen

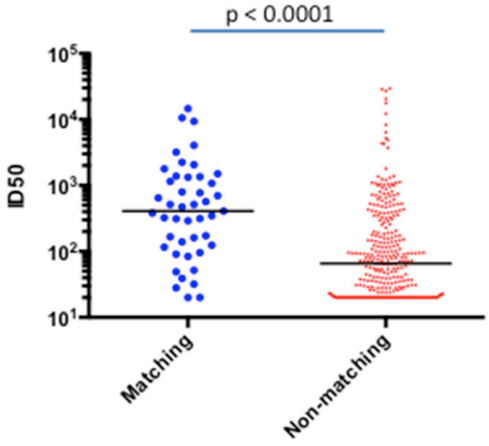

Pseudoviral glycan KO mutants

A

Rabbit and group number	Immunogen BG505 SOSIPv4.1	Tier-2 HIV-1 Env in pseudovirus								
		Ce1176	25710	TRO.11	BJOX2000	X1632	246-F3	CH119	Ce0217	CNE55
		Clade C	Clade C	Clade B	CRF07_BC	Clade B	Clade AC	CRF07_BC	Clade A	CRF01_AE
			N241-	N130+		N332-	N332-			N130+ N332-
2212-1	Parental	22	25	29	61	52	73	67	96	63
2213-1		-	-	-	-	-	-	-	40	-
2214-1		-	-	-	-	-	-	-	-	-
2215-1		26	26	34	60	51	71	75	93	69
2216-1		-	-	-	-	-	-	22	25	22
2217-2	N241-KI	-	-	-	-	-	-	-	-	-
2218-2		-	-	-	-	-	-	-	-	-
2219-2		-	-	-	-	-	-	-	-	-
2220-2		-	-	-	-	-	-	29	32	23
2221-2		-	-	-	-	-	-	-	-	-
2222-3	N241-KI + N130-KI	-	-	-	-	-	-	49	63	-
2223-3		-	-	-	-	-	-	-	25	-
2224-3		-	-	-	-	-	-	-	-	-
2225-3		-	-	-	-	-	-	-	-	60
2226-3		-	-	22	-	-	27	73	56	-
2227-4	N241-KI + N197-KO	-	-	-	-	-	-	21	28	70
2228-4		-	-	-	41	29	-	37	71	-
2229-4		-	-	-	-	-	-	-	40	24
2230-4		-	-	-	-	-	27	31	50	49
2231-4		-	-	-	30	22	62	80	87	54
2232-5	N241-KI + N234-KO	-	-	-	36	27	47	43	58	-
2233-5		-	-	-	-	-	-	-	-	-
2234-5		-	-	-	-	-	-	-	20	28
2235-5		-	-	-	-	-	-	-	40	-
2236-5		-	-	-	-	-	-	-	-	-
2237-6	N241-KI + N276-KO	-	-	-	-	-	-	-	-	-
2238-6		-	-	-	-	-	-	-	-	-
2239-6		-	-	-	-	-	-	-	-	74
2240-6		-	-	-	-	-	33	35	35	-
2241-6		-	-	-	-	-	-	25	30	130
2242-7	N241-KI + N332-KO	-	-	-	55	-	62	85	70	72
2243-7		-	-	-	-	-	29	65	48	35
2244-7		-	-	-	-	-	-	42	44	73
2245-7		-	-	-	23	-	56	58	73	83
2246-7		-	-	-	41	47	22	49	59	-
2247-8	N241-KI + N355-KO	-	-	-	22	-	33	22	24	-
2248-8		-	-	-	-	-	-	-	-	-
2249-8		-	-	-	-	-	-	-	-	70
2250-8		-	-	-	24	-	40	51	82	110
2251-8		-	-	-	72	49	76	86	110	26

B

Rabbit and group	Immunogen B41 SOSIP.v4.1	Tier-2 HIV-1 Env in pseudovirus								
		Ce1176	25710	TRO.11	BJOX2000	X1632	246-F3	CH119	Ce0217	CNE55
		Clade C	Clade C	Clade B	CRF07_BC	Clade B	Clade AC	CRF07_BC	Clade A	CRF01_AE
		N356-				N332- N356-	N332-		N289-	N332-
2256-9	Parental	-	-	-	-	-	-	-	-	-
2257-9		550	160	170	-	50	140	52	-	230
2258-9		72	-	-	-	-	27	22	-	-
2259-9		-	-	-	-	-	-	-	-	-
2260-9		-	-	-	-	-	-	-	-	-
2261-10	N289-KI	-	-	-	-	-	-	-	-	-
2262-10		120	-	-	-	-	-	-	-	30
2263-10		-	-	-	-	-	-	-	-	-
2264-10		120	-	-	-	-	-	-	-	-
2265-10		50	-	-	-	-	-	-	-	22
2266-11	N289-KI + N332-KO	-	-	-	-	-	-	-	-	-
2267-11		150	59	52	-	-	-	-	-	85
2268-11		160	55	51	-	-	-	-	-	120
2269-11		-	-	-	-	-	-	-	-	-
2270-11		-	-	-	-	-	-	-	-	-
2271-12	N289-KI + N356-KO	-	-	-	-	-	-	-	-	-
2272-12		-	-	-	-	-	-	-	-	-
2273-12		-	-	-	-	-	-	-	-	-
2274-12		-	-	-	-	-	-	-	-	-
2275-12		-	-	-	-	-	-	-	-	-

A Figure 5

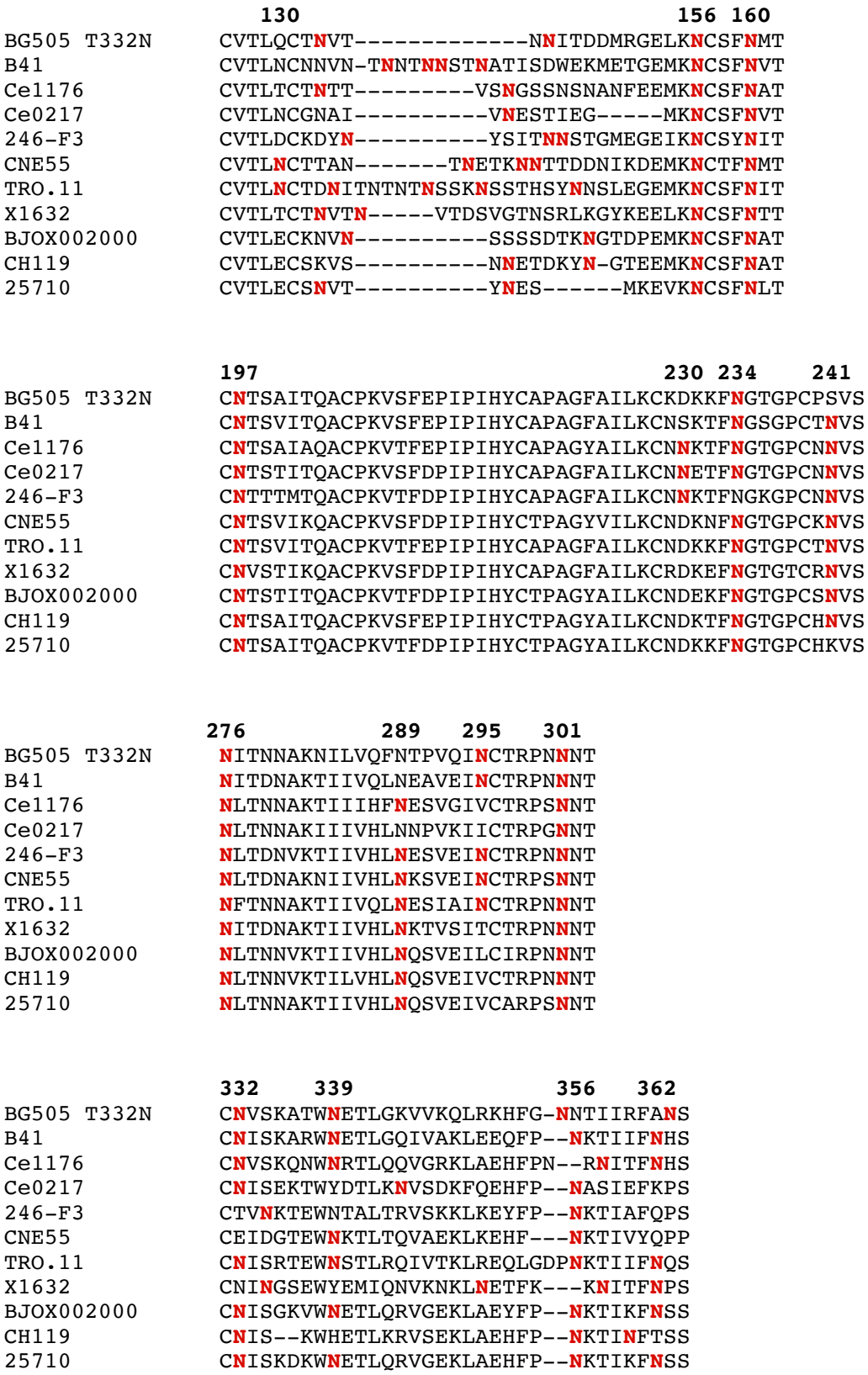
130 156 160
BG505 T332N CVTLQCTNVT----------NNITDDMRGELKNCSFNMT
B41 CVTLNCNNVN-TNNTNNSTNATISDWEKMETGEMKNCSFNVT
Ce1176 CVTLTCTNTT---------VSNGSSNSNANFEEMKNCSFNAT
Ce0217 CVTLNCGNAI----------VNESTIEG-----MKNCSFNVT
246-F3 CVTLDCKDYN----------YSITNNSTGMEGEIKNCSYNIT
CNE55 CVTLNCTTAN-------TNETKNNTTDDNIKDEMKNCTFNMT
TRO.11 CVTLNCTDNITNTNTNSSKNSSTHSYNNSLEGEMKNCSFNIT
X1632 CVTLTCTNVTN-----VTDSVGTNSRLKGYKEELKNCSFNTT
BJOX002000 CVTLECKNVN----------SSSSDTKNGTDPEMKNCSFNAT
CH119 CVTLECSKVS----------NNETDKYN-GTEEMKNCSFNAT
25710 CVTLECSNVT----------YNES------MKEVKNCSFNLT
197 230 234 241
BG505 T332N CNTSAITQACPKVSFEPIPIHYCAPAGFAILKCKDKKFNGTGPCPSVS
B41 CNTSVITQACPKVSFEPIPIHYCAPAGFAILKCNSKTFNGSGPCTNVS
Ce1176 CNTSAIAQACPKVTFEPIPIHYCAPAGYAILKCNNKTFNGTGPCNNVS
Ce0217 CNTSTITQACPKVSFDPIPIHYCAPAGFAILKCNNETFNGTGPCNNVS
246-F3 CNTTTMTQACPKVTFDPIPIHYCAPAGFAILKCNNKTFNGKGPCNNVS
CNE55 CNTSVIKQACPKVSFDPIPIHYCTPAGYVILKCNDKNFNGTGPCKNVS
TRO.11 CNTSVITQACPKVTFEPIPIHYCAPAGFAILKCNDKKFNGTGPCTNVS
X1632 CNVSTIKQACPKVSFDPIPIHYCAPAGFAILKCRDKEFNGTGTCRNVS
BJOX002000 CNTSTITQACPKVTFDPIPIHYCTPAGYAILKCNDEKFNGTGPCSNVS
CH119 CNTSAITQACPKVSFEPIPIHYCTPAGYAILKCNDKTFNGTGPCHNVS
25710 CNTSAITQACPKVTFDPIPIHYCTPAGYAILKCNDKKFNGTGPCHKVS
276 289 295 301
BG505 T332N NITNNAKNILVQFNTPVQINCTRPNNNT
B41 NITDNAKTIIVQLNEAVEINCTRPNNNT
Ce1176 NLTNNAKTIIIHFNESVGIVCTRPSNNT
Ce0217 NLTNNAKIIIVHLNNPVKIICTRPGNNT
246-F3 NLTDNVKTIIVHLNESVEINCTRPNNNT
CNE55 NLTDNAKNIIVHLNKSVEINCTRPSNNT
TRO.11 NFTNNAKTIIVQLNESIAINCTRPNNNT
X1632 NITDNAKTIIVHLNKTVSITCTRPNNNT
BJOX002000 NLTNNVKTIIVHLNQSVEILCIRPNNNT
CH119 NLTNNVKTILVHLNQSVEIVCTRPNNNT
25710 NLTNNAKTIIVHLNQSVEIVCARPSNNT
332 339 356 362
BG505 T332N CNVSKATWNETLGKVVKQLRKHFG-NNTIIRFANS
B41 CNISKARWNETLGQIVAKLEEQFP--NKTIIFNHS
Ce1176 CNVSKQNWNRTLQQVGRKLAEHFPN--RNITFNHS
Ce0217 CNISEKTWYDTLKNVSDKFQEHFP--NASIEFKPS
246-F3 CTVNKTEWNTALTRVSKKLKEYFP--NKTIAFQPS
CNE55 CEIDGTEWNKTLTQVAEKLKEHF---NKTIVYQPP
TRO.11 CNISRTEWNSTLRQIVTKLREQLGDPNKTIIFNQS
X1632 CNINGSEWYEMIQNVKNKLNETFK---KNITFNPS
BJOX002000 CNISGKVWNETLQRVGEKLAEYFP--NKTIKFNSS
CH119 CNIS--KWHETLKRVSEKLAEHFP--NKTINFTSS
25710 CNISKDKWNETLQRVGEKLAEHFP--NKTIKFNSS